

UNCLASSIFIED

AD **298 965**

*Reproduced
by the*

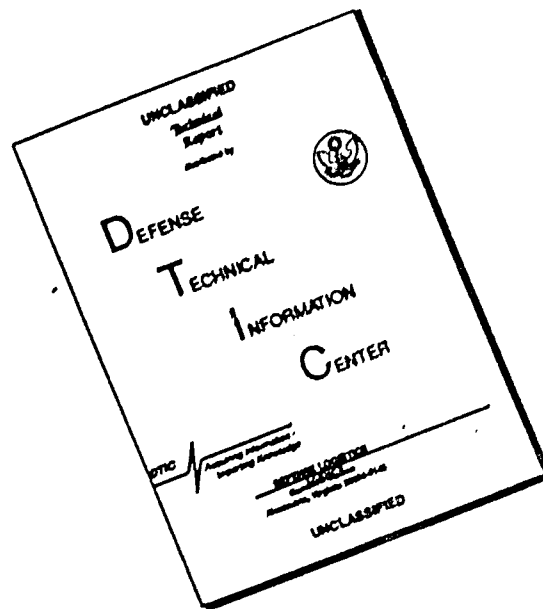
ARMED SERVICES TECHNICAL INFORMATION AGENCY
ARLINGTON HALL STATION
ARLINGTON 12, VIRGINIA



UNCLASSIFIED

NOTICE: When government or other drawings, specifications or other data are used for any purpose other than in connection with a definitely related government procurement operation, the U. S. Government thereby incurs no responsibility, nor any obligation whatsoever; and the fact that the Government may have formulated, furnished, or in any way supplied the said drawings, specifications, or other data is not to be regarded by implication or otherwise as in any manner licensing the holder or any other person or corporation, or conveying any rights or permission to manufacture, use or sell any patented invention that may in any way be related thereto.

DISCLAIMER NOTICE



THIS DOCUMENT IS BEST QUALITY AVAILABLE. THE COPY FURNISHED TO DTIC CONTAINED A SIGNIFICANT NUMBER OF PAGES WHICH DO NOT REPRODUCE LEGIBLY.

SIA 298965
298 965



Radiation Pattern of a Slit in a Ground Plane Covered by a Plasma Layer

MASAYUKI OMURA

Requests for additional copies by Agencies of the Department of Defense, their contractors, and other government agencies should be directed to the:

Armed Services Technical Information Agency
Arlington Hall Station
Arlington 12, Virginia

Department of Defense contractors must be established for ASTIA services, or have their 'need-to-know' certified by the cognizant military agency of their project or contract.

All other persons and organizations should apply to the:

U. S. DEPARTMENT OF COMMERCE
OFFICE OF TECHNICAL SERVICES,
WASHINGTON 25, D. C.



Research Report

Radiation Pattern of a Slit in a Ground Plane Covered by a Plasma Layer

MASAYUKI OMURA

This paper was submitted as a thesis in partial fulfillment of the requirements for the degree of Master of Science of the Massachusetts Institute of Technology and is published with the permission of the Institute.

ELECTROMAGNETIC RADIATION LABORATORY PROJECT 4642

AIR FORCE CAMBRIDGE RESEARCH LABORATORIES, OFFICE OF AEROSPACE RESEARCH, UNITED STATES AIR FORCE, L.G. HANSCOM FIELD, MASS.

Abstract

Expressions for the radiation patterns of a slit in an infinite ground plane covered by a uniform layer of plasma are obtained. The slit is considered to be infinitely long. Two polarizations are considered. In one case, the electric field is polarized across the gap, and in the other, the electric field is polarized along the slit.

The effects of anisotropic plasmas on the radiation pattern are also studied. However, only the non-gyrotropic plasmas are considered.

The solutions to Maxwell's equations are expressed in terms of spectrum of plane waves in the rectangular coordinate system. Fourier transform relations are used to match the boundary conditions. The solutions are obtained in the integral form, and the saddle-point integration method is used to obtain the far-field asymptotic expression of the solutions.

The normalized power patterns are plotted for the various cases studied, and the results discussed.

Contents

Section		Page
	List of Illustrations	vii
	Acknowledgments	ix
1	INTRODUCTION	1
	1. 1 Method of Solution	2
	1. 2 Effective Permittivity of a Plasma Medium	2
	1. 3 Plane Waves	4
2	TRANSVERSE MAGNETIC WAVE	7
	2. 1 Solution in Integral Form	7
	2. 2 Saddle-Point	11
	2. 3 Power Pattern	16
	2. 4 Plane Wave Model and Transmission Line Analogy	20
3	TRANSVERSE ELECTRIC WAVE	26
	3. 1 Solution	26
	3. 2 Results	29
4	ANISOTROPIC PLASMA	33
	4. 1 Introduction	33
	4. 2 Propagation in Anisotropic Medium	33
	4. 3 Solution	36
	4. 4 Results	38
	References	43
	Appendix	45

Illustrations

Figure		Page
1	Plane Wave in Semi-Infinite Medium	5
2	Radiative Geometry for the TM Wave Case	7
3	Electric Field at $z = 0$ for the TM Wave Case	8
4	Complex φ Plane	13
5	Power Patterns for Various Values of $\frac{\omega_p}{\omega}$ (TM Wave Case)	18
6	Power Patterns for Various Values of $k_0 l$ (TM Wave Case)	19
7	Attenuation vs. $\frac{\omega_p}{\omega}$ at $\theta = 0$	20
8	Plane Wave Source	21
9	Plane Wave Source with a Plasma Slab	21
10	Transmission Line Analogue	23
11	Radiative Geometry for the TE Wave Case	26
12	Electric Field Amplitude Distribution at $z = 0$ for the TE Wave Case	26
13	Power Patterns for Various Values of $\frac{\omega_p}{\omega}$ (TE Wave Case)	31
14	Power Patterns for Various Values of $k_0 l$ (TE Wave Case)	31
15	Plane Wave in Anisotropic Medium	35
16	Power Patterns for Various Values of $\frac{\omega_p}{\omega}$ with the Magnetostatic Field in the z Direction	40
17	Power Patterns for Various Values of $\frac{\omega_p}{\omega}$ with the Magnetostatic Field in the x Direction	41

Acknowledgments

The author is indebted to Professor L. J. Chu who spent valuable hours giving advice and guidance. Also, he is grateful to Mr. Walter Rotman of the Missile Antenna Branch, Air Force Cambridge Research Laboratories, for his continued encouragement and active interest in this report.

Radiation Pattern of a Slit in a Ground Plane Covered by a Plasma Layer

1. INTRODUCTION

When a supersonic missile re-enters the earth's atmosphere, it becomes surrounded by a layer of ionized gas. The presence of the ionized gas around the re-entry vehicle alters the performance of the vehicle's radiative system. The effects of the plasma layer on the attenuation and the shape of the antenna pattern are difficult to predict because the plasma layer is highly nonuniform, and the geometry of the radiating structure is not always simple.¹

The object of this report is to study the attenuation and the changes in the far-field radiation pattern due to a plasma layer for a simple radiative system, namely, a slit in an infinite ground plane covered by a uniform layer of plasma. The geometry is a good approximation to either a horn or a slot mounted flush with the body of the re-entry vehicle.

Assuming that the slit is infinitely long, the problem is reduced to a two-dimensional one. The plasma layer is assumed to be uniform and linear.

Two different polarizations are considered. In Section 2, the case of the electric field polarized across the gap is investigated. A limiting case of this particular polarization has been investigated by Newstein and Lurye.² The power patterns are plotted and the features of the patterns are explained in terms of simple models.

In Section 3, the case of the electric field polarized parallel to the slit is studied. Radiation patterns with anisotropic but non-gyrotropic plasma layer are investigated in Section 4.

1.1 Method of Solution

To solve the problem, the solution of Maxwell's equations is expressed as an infinite space spectrum of plane waves in rectangular coordinates. Fourier transform relations are used to match the boundary condition at the ground plane. By applying boundary conditions at the other interface, the solution of the field is expressed as a Fourier integral. Finally, to obtain the far-field radiation pattern, the saddle-point integration method is used to evaluate the integral.

1.2 Effective Permittivity of a Plasma Medium^{3, 8, 9}

In this section, the effective dielectric permittivity for the simplest model of plasma medium is derived, and procedures to obtain the permittivity of more complicated models are indicated.

Plasma is an ionized gas which is electrically neutral. Since the ions are much heavier than the electrons, the velocity of ions due to the applied fields is negligible when compared with the velocity of the electrons in this model. The effect of collision is neglected at first.

Assuming a time dependence of the form $e^{j\omega t}$, Maxwell's equations in complex form are given by:

$$\nabla \times \bar{E} = -j\omega\mu_0 \bar{H} \quad (1.1a)$$

$$\nabla \times \bar{H} = j\omega\epsilon_0 \bar{E} + \bar{J} \quad (1.1b)$$

$$\bar{J} = \rho \bar{v} \quad (1.1c)$$

where ρ is the electron charge density and \bar{v} is the velocity of the electrons. It shall be assumed that the medium being dealt with is homogeneous and that the applied electromagnetic fields are not so large as to change appreciably the homogeneity of the medium. In other words,

$$\rho \approx \rho_0 = \text{constant.}$$

The equation of motion for the electrons is given by

$$m \frac{d\bar{v}}{dt} = e (\bar{E} + \bar{v} \times \mu_0 \bar{H}) \quad (1.2)$$

where e = electron charge and m = electron mass. With the initial assumption that there is no magnetostatic field present, the quantity $\bar{v} \times \mu_0 \bar{H}$ becomes second order and is neglected. The equation of motion in complex form reduces to

$$j\omega m \bar{v} = e \bar{E} \quad (1.3)$$

$$\bar{v} = \frac{e \bar{E}}{j\omega m}$$

Substituting this relation into Eqs. (1.1b) and (1.1c),

$$\begin{aligned}\nabla \times \bar{H} &= j\omega\epsilon_0 \bar{E} + \frac{\rho_0 e}{j\omega m} \bar{E} \\ &= j\omega\epsilon_0 \left[1 - \frac{\rho_0 e^2}{\omega^2 m \epsilon_0} \right] \bar{E} .\end{aligned}\quad (1.4)$$

But $\rho_0 = N_0 e$ where N_0 is the electron density. Therefore,

$$\nabla \times \bar{H} = j\omega\epsilon_0 \left[1 - \frac{N_0 e^2}{\omega^2 m \epsilon_0} \right] \bar{E} .\quad (1.5)$$

This gives the effective dielectric constant of

$$\epsilon_p = \epsilon_0 \left[1 - \frac{N_0 e^2}{\omega^2 m \epsilon_0} \right] = \epsilon_0 \left[1 - \frac{\omega_p^2}{\omega^2} \right] ,\quad (1.6)$$

where $\omega_p^2 = \frac{N_0 e^2}{m \epsilon_0} .$

Since the velocity of the electrons is 90° out of phase with the applied electric field, there is no loss [see Eq. (1.3)]. When the effect of collisions is appreciable, the velocity of the electrons is no longer 90° out of phase with the applied field. The effect of collisions is included in the equation of motion as a damping term given below:

$$m \frac{d\bar{v}}{dt} + m\nu\bar{v} = e\bar{E} \quad (1.7)$$

where ν is the collision frequency. For such a system, the permittivity is given by

$$\epsilon_p = \epsilon_0 \left[1 - \frac{\omega_p^2}{\nu^2 + \omega^2} + j \frac{\nu}{\omega} \frac{\omega_p^2}{\nu^2 + \omega^2} \right] .\quad (1.8)$$

Macroscopically, the important difference between an ordinary dielectric and a plasma medium is that the real part of the permittivity for the plasma medium is less than ϵ_0 . Actually, the real part of ϵ_p can take on negative values.

If a magnetostatic field is introduced, then the equation of motion for the electrons becomes

$$m \frac{d\bar{v}}{dt} + m\nu\bar{v} = e \left[\bar{E} + \bar{v} \times \bar{B}_0 \right] .\quad (1.9)$$

Such an equation of motion gives rise to a tensor permittivity of the following form (in the rectangular coordinate system):

$$\begin{bmatrix} 1 + \frac{\nu + j\omega}{(\nu + j\omega)^2 + \omega_b^2} \left(\frac{\omega_p^2}{j\omega} \right) & \frac{\omega_b}{(\nu + j\omega)^2 + \omega_b^2} \left(\frac{\omega_p^2}{j\omega} \right) & 0 \\ \frac{-\omega_b}{(\nu + j\omega)^2 + \omega_b^2} \left(\frac{\omega_p^2}{j\omega} \right) & 1 + \frac{(\nu + j\omega)}{(\nu + j\omega)^2 + \omega_b^2} \left(\frac{\omega_p^2}{j\omega} \right) & 0 \\ 0 & 0 & 1 + \frac{\omega_p^2}{(\nu + j\omega)(j\omega)} \end{bmatrix}.$$

The magnetostatic field is assumed to be in the z direction in a right-hand coordinate system. The quantity ω_b is the gyrofrequency and is defined as:

$$\omega_b = \frac{eB_0}{m}.$$

1.3 Plane Waves

In the analysis of the radiation problem, the fields are expanded in terms of plane waves. A brief review of plane waves in semi-infinite medium is given here. In the subsequent analysis, the time dependence $e^{j\omega t}$ is assumed.

From Maxwell's equations, the following equation, known as Helmholtz equation, can be obtained for the electric field:

$$[\nabla^2 + \mu\epsilon\omega^2] \vec{E} = 0,$$

where for the rectangular coordinate system

$$\nabla^2 = \frac{\partial^2}{\partial x^2} + \frac{\partial^2}{\partial y^2} + \frac{\partial^2}{\partial z^2}. \quad (1.10)$$

In general, the solution to such an equation in rectangular coordinate system is given by:

$$E_{(x,y,z)} = A_0 (e^{-jk_x x} + \Gamma_1 e^{jk_x x}) (e^{-jk_y y} + \Gamma_2 e^{jk_y y}) (e^{-jk_z z} + \Gamma_3 e^{jk_z z}),$$

where

$E_{(x,y,z)}$ = a component of electric field

A_0 , Γ_1 , Γ_2 , and Γ_3 are complex constants (1.11)

$$k_x^2 + k_y^2 + k_z^2 = \omega^2 \mu \epsilon.$$

Consider the geometry shown in Figure 1. Assume that a uniform plane wave impinges upon the semi-infinite isotropic dielectric from a direction making an angle θ with z axis, and that the electric field is polarized in the y direction. With these simplifications, the solution in the free space region reduces to

$$E_y = A' [e^{-jk_z z} + \Gamma e^{jk_z z}] e^{-jk_x x}, \quad (1.12)$$

where

A' = constant

Γ = reflection coefficient

$$k_y^2 + k_z^2 = \omega^2 \mu_0 \epsilon_0 = k_0^2$$

$$k_y = k_0 \sin \theta$$

$$k_z = k_0 \cos \theta$$

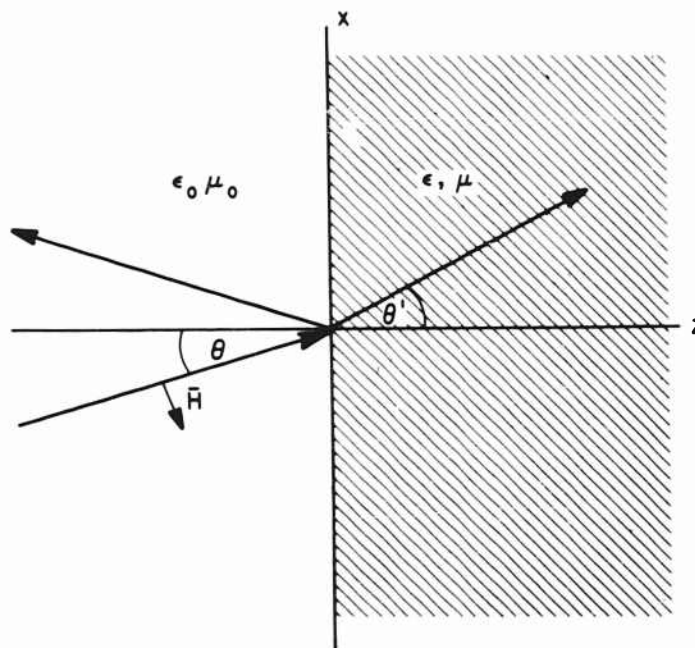


Figure 1. Plane Wave in Semi-Infinite Medium

The first term in Eq. (1.12) represents the wave coming toward the dielectric wall and the second term represents the reflected wave. From Maxwell's equations the magnetic field components H_x and H_z are obtained:

$$H_x = \frac{-1}{j\omega\mu_0} \frac{\partial E_y}{\partial z} = \frac{k_z}{\omega\epsilon_0} A' \left[e^{-jk_z z} - \Gamma e^{jk_z z} \right] e^{-jk_x x}, \quad (1.13)$$

and

$$H_z = \frac{1}{j\omega\mu_0} \frac{\partial E_y}{\partial x} = \frac{-k_x}{\omega\mu_0} A' \left[e^{-jk_z z} + \Gamma e^{jk_z z} \right] e^{-jk_x x}. \quad (1.14)$$

For this particular polarization, all other field components are zero.

Inside the dielectric medium there is no reflected wave. Thus, the expression for the electric field is given by

$$E_y' = T e^{-j(k_x' x + k_z' z)},$$

where

$T = \text{constant}$

$$k_x'^2 + k_z'^2 = k^2 = \omega^2 \mu \epsilon$$

$$k_x' = k \sin \theta'$$

$$k_z' = k \cos \theta'.$$

(1.15)

Again the magnetic field can be obtained from Maxwell's equations. From the boundary conditions, the value of Γ and T can be obtained, as well as the relation between θ and θ' .

For a more detailed analysis of plane waves see Reference 4.

In this problem, the solution to Maxwell's equations will be expressed in terms of plane waves like those of Eqs. (1.12) and (1.15).

In the anisotropic case, there is a different relation between k_x' and k_z' . A discussion of plane waves in an anisotropic medium is given in Section 4.

2. TRANSVERSE MAGNETIC WAVE

2.1 Solution in Integral Form

The geometry for the first problem considered is shown in Figure 2. At the gap, the electric field is polarized in the x direction and the amplitude distribution along the gap is assumed to be constant, as illustrated in Figure 3. The magnetostatic field is assumed to be zero.

A very similar problem, namely that of a magnetic line source in the ground plane covered by a layer of plasma, has been solved by Newstein and Lurye.² The magnetic line source in a ground plane is a limiting case of a slit in a ground plane with the slit becoming infinitesimally narrow.

Contrary to Newstein and Lurye's² method of expanding the solution to Maxwell's equations in terms of cylindrical waves, the solution in this report is expanded in terms of plane waves in rectangular coordinates. However, the results are the same.

It is clear from the boundary conditions that for the particular geometry and polarization described in Figures 2 and 3 that

$$E_y = H_x = H_z = 0$$

$$E'_y = H'_x = H'_z = 0$$

where the primed quantities represent the electric and magnetic fields within the plasma and the unprimed quantities represent the fields in free space.

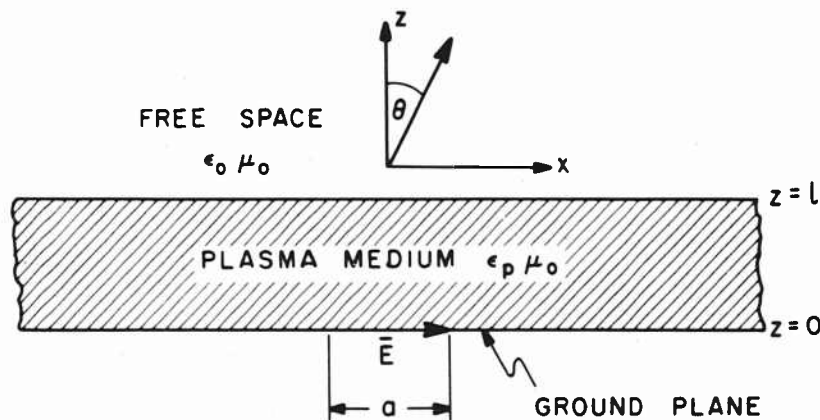


Figure 2. Radiative Geometry for the TM Wave Case

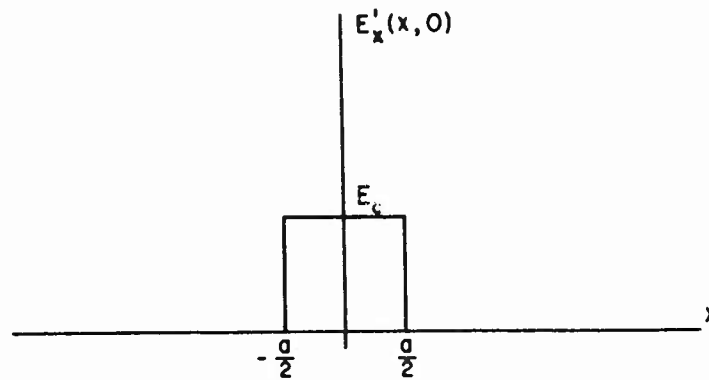


Figure 3. Electric Field at $z = 0$ for the TM Wave Case

In the free space region $z > 1$, the following solution is assumed for the magnetic field:

$$H_y(x, z) = \int_{-\infty}^{\infty} a(k_x) e^{-j(k_x x + k_z z)} dk_x,$$

where $k_z = \pm \sqrt{k_0^2 - k_x^2}$. (2.1)

$a(k_x)$ = amplitude function independent of x and z . Thus, the solution is expressed as a spectrum of outward-going plane waves. If a plane wave satisfies Maxwell's equations, then certainly the sum, or more precisely, the integral of such plane waves satisfies Maxwell's equations.

It should be noted here that along the path of integration, as k_x goes from minus infinity to plus infinity, the quantity k_z takes on both real and

imaginary values. The sign of k_z must be chosen in such a way that the imaginary part of k_z is always negative. If the positive values are taken for the imaginary part, the integral is expressed in terms of increasing exponentials, and the integral will not converge. Physically such a result is not expected.

From Maxwell's equations result the following expressions for the electric field:

$$E_x(x, z) = \frac{-1}{j\omega\epsilon_0} \frac{\partial H_y}{\partial z} = \int_{-\infty}^{\infty} \frac{k_z}{\omega\epsilon_0} a(k_x) e^{-j(k_x x + k_z z)} dk_x, \quad (2.2)$$

$$E_z(x, z) = \frac{1}{j\omega\epsilon_0} \frac{\partial H_y}{\partial x} = \int_{-\infty}^{\infty} \frac{k_x}{\omega\epsilon_0} a(k_x) e^{-j(k_x x + k_z z)} dk_x. \quad (2.3)$$

Inside the plasma medium, the solution for the magnetic field is represented by a spectrum of outward-going waves plus reflected waves as follows:

$$H'_y(x, z) = \int_{-\infty}^{\infty} \left[b(k'_x) e^{-jk'_z z} + c(k'_x) e^{jk'_z z} \right] e^{-jk'_x x} dk'_x, \quad (2.4)$$

where

$$k'_z = (k_p^2 - k'^2_x)^{\frac{1}{2}}$$

$$k_p = \omega \sqrt{\mu_0 \epsilon_p}.$$

The propagation constant k_p is in general a complex quantity. The quantities $b(k'_x)$ and $c(k'_x)$ give the complex amplitudes of outgoing and reflected waves.

The corresponding electric field is obtained from Maxwell's equations:

$$E'_x(x, z) = \frac{-1}{j\omega\epsilon_p} \frac{\partial H'_y}{\partial z} = \int_{-\infty}^{\infty} \frac{k'_z}{\omega\epsilon_p} \left[b(k'_x) e^{-jk'_z z} - c(k'_x) e^{jk'_z z} \right] e^{-jk'_x x} dk'_x. \quad (2.5)$$

$$E'_z(x, z) = \frac{1}{j\omega\epsilon_p} \frac{\partial H'_y}{\partial x} = - \int_{-\infty}^{\infty} \frac{k'_x}{\omega\epsilon_p} \left[b(k'_x) e^{-jk'_z z} + c(k'_x) e^{jk'_z z} \right] e^{-jk'_x x} dk'_x. \quad (2.6)$$

There are three unknowns in this problem: $a(k_x)$, $b(k'_x)$, and $c(k'_x)$. To evaluate them, it is necessary to have three equations relating these quantities. The boundary conditions will provide the necessary relations.

Consider the boundary condition at the ground plane. Here the amplitude of the tangential component of electric field E'_x , as function of x is as shown in Figure 3.

Equation (2.5) for E'_x reduces to the following at $z = 0$:

$$E'_x(x, 0) = \int_{-\infty}^{\infty} \frac{k'_z}{\omega \epsilon_p} \left[b(k'_x) - c(k'_x) \right] e^{-jk'_x x} dk'_x \quad (2.7)$$

Equation (2.7) is a familiar expression for the Fourier transform between the k'_x domain and the x domain. It can be seen readily that the quantity

$$\frac{k'_z}{\omega \epsilon_p} \left[b(k'_x) - c(k'_x) \right]$$

is the Fourier transform of the electric field amplitude distribution, $E'_x(x, 0)$. The Fourier transform of a rectangular pulse is a simple one, and thus, the transform will be equated to the above expression.

$$\frac{k'_z}{\omega \epsilon_p} \left[b(k'_x) - c(k'_x) \right] = \frac{2\pi E_0 a \sin k'_x \frac{a}{2}}{k'_x \frac{a}{2}} \quad (2.8)$$

Equation (2.8) gives one of the three required relations, and the other two relations are obtained at the interface between the plasma and the free space.

At the interface both the tangential component of electric field and that of magnetic field must be continuous. For the magnetic field, Eqs. (2.1) and (2.4) at $z = 1$ can be equated to obtain:

$$\begin{aligned} \int_{-\infty}^{\infty} a(k'_x) e^{-jk'_z 1} e^{-jk'_x x} dk'_x \\ = \int_{-\infty}^{\infty} \left[b(k'_x) e^{-jk'_z 1} + c(k'_x) e^{jk'_z 1} \right] e^{-jk'_x x} dk'_x \end{aligned} \quad (2.9)$$

Similarly, for the tangential component of electric field Eqs. (2.2) and (2.5) can be equated and thus,

$$\begin{aligned} \int_{-\infty}^{\infty} \frac{k'_z}{\epsilon_0} a(k'_x) e^{-jk'_z 1} e^{-jk'_x x} dk'_x \\ = \int_{-\infty}^{\infty} \frac{k'_z}{\epsilon_p} \left[b(k'_x) e^{-jk'_z 1} - c(k'_x) e^{jk'_z 1} \right] e^{-jk'_x x} dk'_x \end{aligned} \quad (2.10)$$

It can be shown that, in order for Eqs. (2.9) and (2.10) to hold, the quantity k'_x must be equal to k_x . This result is not surprising because it shows that the phase must be continuous at the boundary, which is also the requirement from Snell's law. Since the integral now has the same variable, the quantities inside the integral can be equated, noting that:

$$\begin{aligned}
 k_x &= k'_x \\
 k'_z &= \sqrt{k_p^2 - k_x^2} \\
 k_z &= \sqrt{k_0^2 - k_x^2}
 \end{aligned}$$

Thus, from Eqs. (2.9) and (2.10) results:

$$a(k_x) e^{-jk_z l} = b(k'_x) e^{-jk'_z l} + c(k'_x) e^{jk'_z l}, \quad (2.11)$$

and

$$\frac{k_z}{\epsilon_0} a(k_x) e^{-jk_z l} = \frac{k'_z}{\epsilon_p} \left[b(k'_x) e^{-jk'_z l} - c(k'_x) e^{jk'_z l} \right]. \quad (2.12)$$

Equations (2.8), (2.11), and (2.12) give three equations relating the three unknowns. In solving the equations for $a(k_x)$,

$$a(k_x) = \frac{2\pi E_0 a \sin k'_x \frac{a}{2}}{k_z \left(k'_x \frac{a}{2} \right)} \left[\frac{e^{jk'_z l}}{\cos k'_z l + j \frac{k'_z \epsilon_0}{k_z \epsilon_p} \sin k'_z l} \right]. \quad (2.13)$$

Since k'_x , k_z , and k'_z can be expressed in terms of k_x , the right-hand side of Eq. (2.13) can be expressed completely in terms of k_x .

The exact solution in integral form has now been obtained [see Eq. (2.1)]. Evaluation of this integral for large values of x and z by the saddle-point method is used to obtain the asymptotic expression for the far-field radiation pattern.

2.2 Saddle-Point Method

The saddle-point integration method, also known as the method of steepest descent, is a technique to obtain an asymptotic approximation for large values of z to complex integrals of the type

$$\int_c g(s) e^{zf(s)} ds$$

where $g(s)$ and $f(s)$ are independent of z .

In this problem, it is more convenient to change from the rectangular coordinate system to cylindrical coordinates. Thus,

$$\begin{aligned}
 k_x &= k_0 \sin \varphi \\
 k_z &= k_0 \cos \varphi \\
 dk_x &= \frac{dk_x}{d\varphi} d\varphi = k_0 \cos \varphi d\varphi
 \end{aligned}$$

$$\begin{aligned}
 x &= r \sin \theta \\
 x &= r \cos \theta \\
 a(k_x) &= a(k_0 \sin \varphi)
 \end{aligned}$$

where φ , the new variable of integrations, refers to the direction of wave propagation, whereas θ refers to the angle of observation point. Although both θ and φ are measured from the z axis, θ is independent of φ just as x is independent of k_x in the integration.

Substitute these quantities into the integral

$$H_y = \int_{-\infty}^{\infty} a(k_x) e^{-j(k_x x + k_z z)} dk_x$$

and obtain

$$\begin{aligned}
 H_y &= \int_C a(k_0 \sin \varphi) k_0 \cos \varphi e^{-jk_0 r (\cos \varphi \cos \theta + \sin \varphi \sin \theta)} d\varphi \\
 &= \int_C a(k_0 \sin \varphi) k_0 \cos \varphi e^{-jk_0 r [\cos(\theta - \varphi)]} d\varphi \quad (2.14)
 \end{aligned}$$

As the original variable of integration k_x goes from minus infinity to plus infinity; the new variable φ takes the path C shown in Figure 4. The shaded area in Figure 4 is the mapping of the proper sheet of the k_x plane into the complex φ plane. When mapping the k_x plane into the φ plane, it must be noted that the imaginary part of

$$k_z = k_0 \cos \varphi$$

must be negative for the reason of convergence. This condition is satisfied in the shaded region.

The next step of this procedure is to distort the path of integration. If the path C is continuously deformed into another path B in such a way that it does not sweep over a singularity of the integrand, then

$$\int_C = \int_B$$

In order for the integral to converge, it is also required that the two ends of the path stay within the shaded region.

The object of the saddle-point method is to choose a path of integration so that the quantity

$$\exp \left[R_e (-jk_0 r \cos \{ \theta - \varphi \}) \right]$$

has a maximum or more precisely a saddle-point, and falls as rapidly as possible on either side of this maximum. Also along the path near the maxi-

imum the imaginary part of $-jk_0 r \cos(\theta - \varphi)$ is to be constant, or in other words, the phase of the quantity

$$e^{-jk_0 r \cos(\theta - \varphi)}$$

is to be constant along the path. This second condition insures that the integrand does not fluctuate rapidly between positive and negative values.

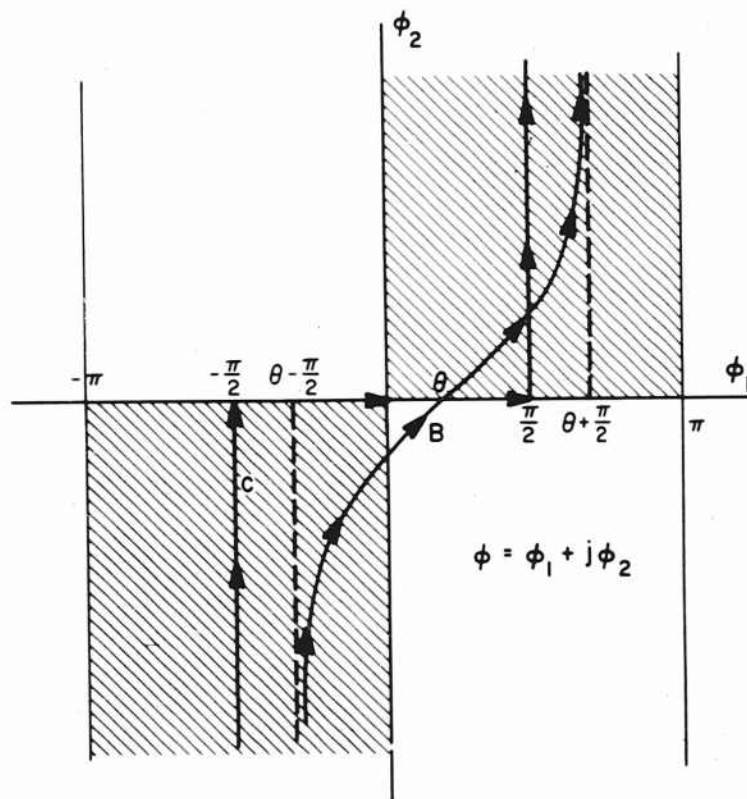


Figure 4. Complex φ Plane

The saddle-point occurs when

$$\frac{\partial}{\partial \varphi} \left[-jk_0 r \cos(\theta - \varphi) \right] = 0$$

or, in other words, at $\varphi = \theta$.

If

$$\varphi = \varphi_1 + j\varphi_2,$$

then

$$-jk_0 r \cos(\theta - \varphi_1 - j\varphi_2) = k_0 r \left[\sinh \varphi_2 \sin(\theta - \varphi_1) - j \cosh \varphi_2 \cos(\theta - \varphi_1) \right]. \quad (2.15)$$

The imaginary part of Eq. (2.15) is to be constant along the new path, and the constant can be evaluated at the saddle-point $\varphi_1 = \theta$, $\varphi_2 = 0$. This gives the equation for the path

$$\cosh \varphi_2 \cos(\theta - \varphi_1) = 1. \quad (2.16)$$

It should be noted that in the range $-\pi < \varphi_1 < \pi$, there is more than one possible path which satisfies Eq. (2.16), but only one stays within the allowed region in the complex φ plane. From Eq. (2.16), therefore,

$$\cos(\theta - \varphi_1) = (\cosh \varphi_2)^{-1}, \quad (2.17a)$$

and

$$\sin(\theta - \varphi_1) = \pm \left[1 - \cos^2(\theta - \varphi_1) \right]^{\frac{1}{2}} = \pm \tanh \varphi_2. \quad (2.17b)$$

The minus sign must be taken in front of $\tanh \varphi_2$ in order to stay on the allowed region.

If Eqs. (2.16) and (2.17b) are substituted into Eq. (2.15), then,

$$-jk_0 r \cos(\theta - \varphi) = -k_0 r \left[\frac{\sinh^2 \varphi_2}{\cosh \varphi_2} + j \right]. \quad (2.18)$$

Now there is a new variable φ_2 which goes from minus infinity to infinity.

It can be seen that if r is very large, the quantity

$$\exp \left[-k_0 r \frac{\sinh^2 \varphi_2}{\cosh \varphi_2} \right]$$

has a maximum at $\varphi_2 = 0$ and decreases very rapidly on either side of the saddle-point. Thus, the major contribution to the original integral comes from a small region of the path near the saddle-point. Therefore, the following approximations near the saddle-point may be made:

$$\frac{\sinh^2 \varphi_2}{\cosh \varphi_2} \approx \varphi_2^2$$

and

$$\begin{aligned} d\varphi &= \frac{\partial \varphi}{\partial \varphi_1} d\varphi_1 + \frac{\partial \varphi}{\partial \varphi_2} d\varphi_2 \\ &= \left[\frac{\partial \varphi}{\partial \varphi_1} \frac{\partial \varphi_1}{\partial \varphi_2} + \frac{\partial \varphi}{\partial \varphi_2} \right] d\varphi_2 \\ &\approx [1 + j] d\varphi_2 = \sqrt{2} e^{j\pi/4} d\varphi_2 . \end{aligned}$$

By inserting these relations into Eqs. (2.18) and (2.14), it can be seen that the major portion of the integral is given by

$$H_y \approx \sqrt{2} e^{j\pi/4} \int_{-u}^u a(k_0 \sin \varphi) k_0 \cos \varphi e^{-jk_0 r} e^{-k_0 r \varphi_2^2} d\varphi_2 \quad (2.19)$$

where u is a point on the path near enough to the saddle-point so that

$$\frac{\sinh^2 u}{\cosh u} \approx u^2$$

is a valid assumption.

If r is made very large, the region $-u < \varphi_2 < u$ can be made very small and still be a good approximation to the integral. If the region $-u < \varphi_2 < u$ is small, the following further approximation within the region can be made:

$$a(k_0 \sin \varphi) \cos \varphi \approx a(k_0 \sin \theta) \cos \theta .$$

The quantity

$$a(k_0 \sin \theta) \cos \theta$$

can now be taken outside the integral and the integral reduces to

$$H_y \approx \sqrt{2} e^{j\pi/4} k_0 \cos \theta a(k_0 \sin \theta) e^{-jk_0 r} \int_{-u}^u e^{-k_0 r \varphi_2^2} d\varphi_2 . \quad (2.20)$$

It can be seen that if the limits of integration are extended from minus infinity to plus infinity, the value of the integral changes very little because r is assumed to be very large. Thus the integral is approximated further to the following:

$$H_y \approx \sqrt{2} e^{j\pi/4} k_0 \cos \theta a(k_0 \sin \theta) e^{-jk_0 r} \int_{-\infty}^{\infty} e^{-k_0 r \varphi_2^2} d\varphi_2 . \quad (2.21)$$

The integral above is a well-known definite integral and thus the approximate solution is

$$H_y \approx \sqrt{\frac{2\pi}{k_0 r}} e^{j\pi/4} k_0 \cos \theta a(k_0 \sin \theta) e^{-jk_0 r},$$

where

$$a(k_0 \sin \theta) = \frac{2\pi E_0 a \sin(\frac{k_0 a}{2} \sin \theta)}{k_0 \cos \theta \frac{k_0 a}{2} \sin \theta} \left[\frac{e^{jk_0 l \cos \theta}}{\cos k'_z l + j \frac{\epsilon_0 k'_z}{\epsilon_p k_0 \cos \theta} \sin k'_z l} \right] \quad (2.22)$$

$$k'_z = \sqrt{k_p^2 - k_0^2 \sin^2 \theta}.$$

In the analysis, the effect of poles of integrand in the complex φ plane has been disregarded. The contribution from the poles can be included in the usual manner, but can be neglected in the far-field analysis of r approaching infinity unless the pole lies on the real axis of the φ plane. In this problem there was no pole on the real axis, and thus the analysis is valid.

The expression for the electric field can be obtained in a similar manner. If E_x and E_z are combined to obtain a single component E_θ , then

$$E_\theta = \sqrt{\frac{\mu_0}{\epsilon_0}} H_y. \quad (2.23)$$

2.3 Power Pattern

The power pattern can now be obtained from the relation

$$P = \frac{1}{2} \sqrt{\frac{\mu_0}{\epsilon_0}} |H_y|^2.$$

For the case of lossy plasma layer, the expression for the power pattern becomes quite complicated. A useful form of power pattern cannot be obtained for such a case, and thus only the expression for lossless plasma will be given here. However, the equations for the lossy plasma cases are presented in the Appendix.

Since the quantity k'_z in Eq. (2.22) takes on real and imaginary values for the lossless case, it is convenient to give two expressions for power pattern; one valid when k'_z is real, and the other valid when k'_z is imaginary.

Let

$$k'_{zr} = \sqrt{k_p^2 - k_0^2 \sin^2 \theta}$$

$$k'_{zi} = \sqrt{k_0^2 \sin^2 \theta - k_p^2},$$

where

$$k_p^2 = k_0^2 \left[1 - \frac{\omega_p^2}{\omega^2} \right].$$

Then

$$k'_z = k'_{zr} \quad \text{for } \cos \theta > \frac{\omega_p}{\omega},$$

and

$$k'_z = jk'_{zi} \quad \text{for } \cos \theta < \frac{\omega_p}{\omega}.$$

It should be noted that when the plasma layer is lossy, the quantity k'_z is complex instead of pure real or pure imaginary.

By substituting the relations above for k'_z into Eq. (2.22), the following expressions for the normalized power pattern are obtained:

$$P_n = \frac{1}{r} \left[\frac{\sin\left(\frac{k_0 a}{2} \sin \theta\right)}{\frac{k_0 a}{2} \sin \theta} \right]^2 \left[\frac{1}{\cos^2 k'_{zr} + \frac{\epsilon_0^2 k'^2_{zr}}{\epsilon_p^2 k_0^2 \cos^2 \theta} \sin^2 k'_{zr}} \right] \quad (2.24a)$$

for

$$\cos \theta > \frac{\omega_p}{\omega}$$

and

$$P_n = \frac{1}{r} \left[\frac{\sin\left(\frac{k_0 a}{2} \sin \theta\right)}{\frac{k_0 a}{2} \sin \theta} \right]^2 \left[\frac{1}{\cosh^2 k'_{zi} + \frac{\epsilon_0^2 k'^2_{zi}}{\epsilon_p^2 k_0^2 \cos^2 \theta} \sinh^2 k'_{zi}} \right] \quad (2.24b)$$

for

$$\cos \theta < \frac{\omega_p}{\omega}.$$

In normalizing the power pattern, it was assumed that the voltage across the gap is constant for all cases.

Since $\cos^2 \theta$ is never greater than unity, only Eq. (2.24b) is needed when $\frac{\omega_p}{\omega}$ is greater than unity. However, when $\frac{\omega_p}{\omega} < 1$ there is a definite angle at which k'_z changes from real to imaginary quantity. This angle will be called the cutoff angle. The cutoff angle is given by

$$\theta_c = \cos^{-1} \frac{\omega_p}{\omega}.$$

In Figures 5 and 6, some radiation patterns are plotted. In plotting them, it was assumed that the slit was infinitesimally narrow. This assumption gives the relation

$$\frac{\frac{k_0 a}{2} \sin \theta}{\frac{k_0 a}{2} \sin \theta} = 1.$$

In Figure 5, power patterns are shown for various values of $\frac{\omega_p}{\omega}$ with fixed plasma thickness. The cutoff angles are indicated on the graph. An interesting feature of the patterns is that when $\frac{\omega_p}{\omega} < 1$, the patterns have peaks just inside the cutoff angle. For the values of θ greater than the cutoff angle, the amplitudes decrease rapidly with increase in the angle.

When $\frac{\omega_p}{\omega} > 1$, the amplitudes of the pattern are greatly attenuated. This effect is due to the propagation constant in the plasma given by the expression

$$k_p = k_0 \left[1 - \left(\frac{\omega_p}{\omega} \right)^2 \right]^{\frac{1}{2}}$$

which becomes imaginary. Thus the waves are attenuated exponentially within the plasma layer.

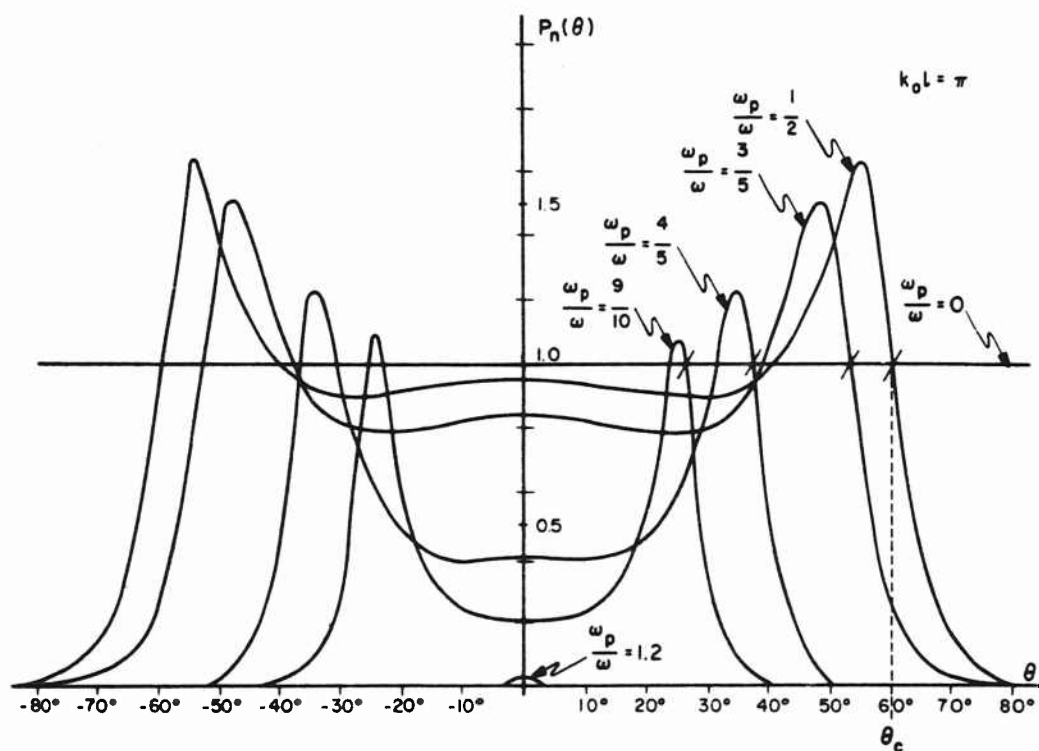


Figure 5. Power Patterns for Various Values of $\frac{\omega_p}{\omega}$ (TM Wave Case)

Figure 6 shows the power patterns plotted as functions of plasma layer thickness. For the particular value of $\frac{\omega_p}{\omega}$ chosen, the cutoff angle was 37° . Since the power patterns are symmetric in θ , only half of each pattern is plotted. The peaks fall approximately at the same angle and they are higher for thicker plasma layers.

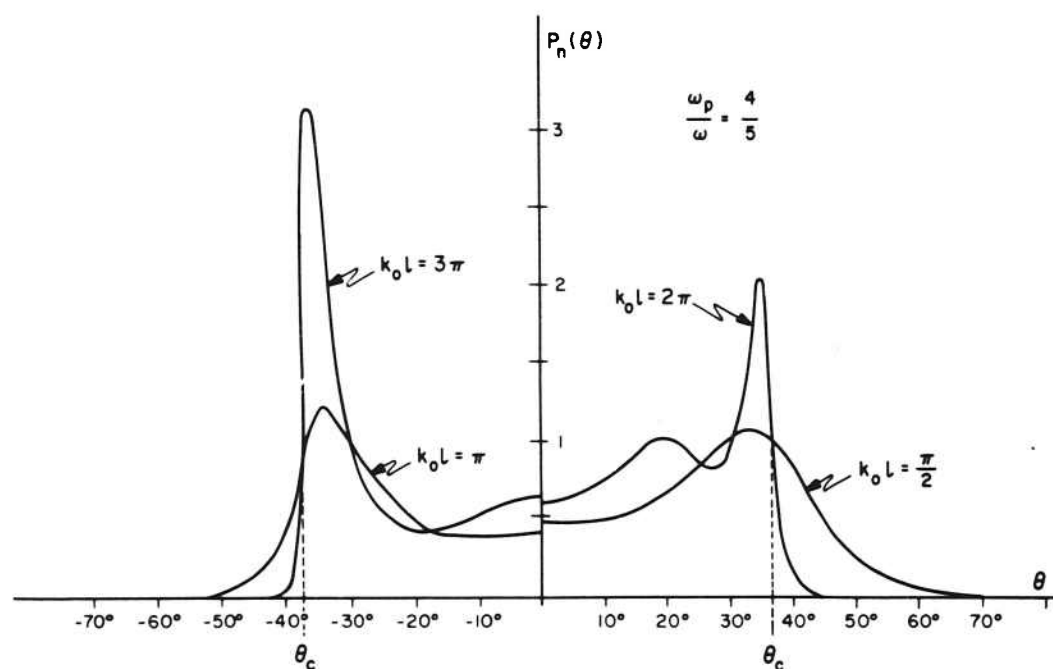


Figure 6. Power Patterns for Values of $k_0 l$ (TM Wave Case)

Since the ground plane is never infinite in practice, an important relation is the attenuation as a function of $\frac{\omega_p}{\omega}$ for $\theta = 0$. The plot of attenuation versus $\frac{\omega_p}{\omega}$ with the plasma thickness as a parameter is given in Figure 7.

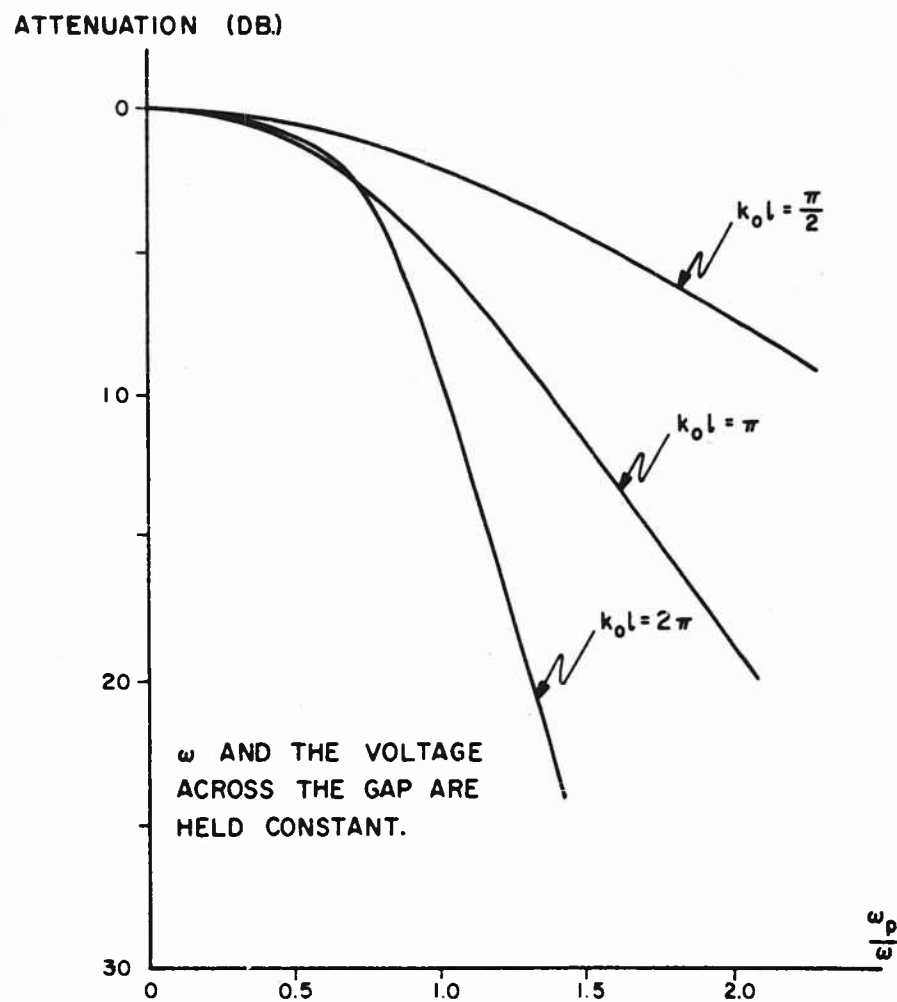


Figure 7. Attenuation vs. $\frac{\omega_p}{\omega}$ at $\theta = 0$

2.4 Plane Wave Model and Transmission Line Analogy

To get some physical feeling for the problem, consider the following system.

Let a fictitious plane wave source at $z = 0$ which constrains the x component of the electric field to be of the form

$$e_x(z=0) = E_0 \cos \theta e^{-jk_0 x \sin \theta},$$

where $k_0 = \omega \sqrt{\mu_0 \epsilon_0}$. (Small letters are used to denote the field components for the plane wave model.)

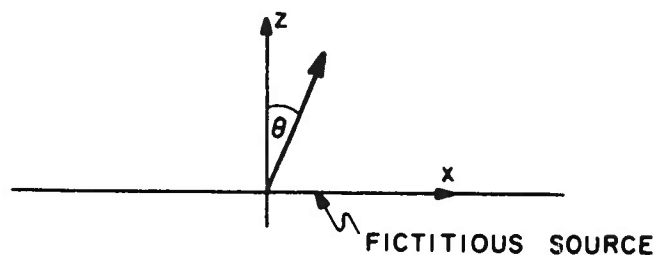


Figure 8. Plane Wave Source

If freedom to choose θ is assumed, and the source extends from $x = -\infty$ to $x = \infty$, then such a source propagates a plane wave in the θ direction with the magnetic field given by:

$$\vec{h} = E_0 \sqrt{\frac{\epsilon_0}{\mu_0}} e^{-jk_0(x \sin \theta + z \cos \theta)} \vec{i}_y \quad (2.25)$$

Thus for any θ the choice is between $-\pi/2$ and $\pi/2$; the source propagates a plane wave with the electric field amplitudes equal to E_0 .

Now suppose that a slab of plasma is placed against the source as shown in Figure 9.

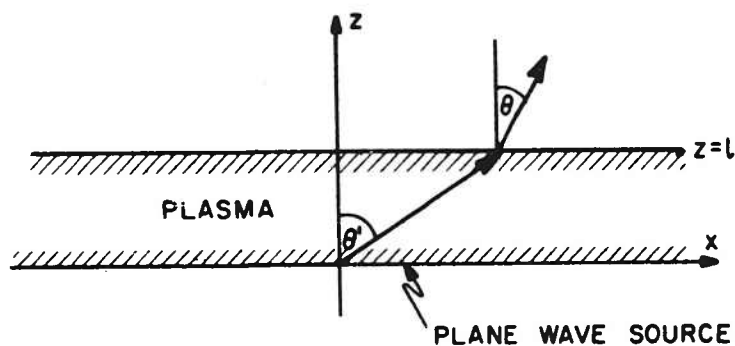


Figure 9. Plane Wave Source with a Plasma Slab

To solve for the fields, assume plane wave solutions in the two regions of interest. Inside the plasma layer there is a solution of the following form:

$$h'_y = H'_0 \left[e^{-jk'_z z + \Gamma e^{jk'_z z}} \right] e^{-jk'_x x} \quad (2.26a)$$

$$e'_x = \frac{-1}{j\omega\epsilon_p} \frac{\partial h'_y}{\partial z} = \frac{H'_0 k'_z}{\omega\epsilon_p} \left[e^{-jk'_z z} - \Gamma e^{jk'_z z} \right] e^{-jk'_x x} \quad (2.26b)$$

$$e'_z = \frac{1}{j\omega\epsilon_p} \frac{\partial h'_y}{\partial x} = \frac{-H'_0 k'_x}{\omega\epsilon_p} \left[e^{-jk'_z z} + \Gamma e^{jk'_z z} \right] e^{-jk'_x x} \quad (2.26c)$$

where

$$k'_x = k_p \sin \theta'$$

$$k'_z = k_p \cos \theta'.$$

In the region $z > 1$,

$$h_y = H_0 e^{-j(k_z z + k_x x)} \quad (2.27a)$$

$$e_x = \frac{H_0 k_z}{\omega\epsilon_0} e^{-j(k_z z + k_x x)} \quad (2.27b)$$

$$e_z = \frac{-H_0 k_x}{\omega\epsilon_0} e^{-j(k_z z + k_x x)} \quad (2.27c)$$

where

$$k_x = k_0 \sin \theta$$

$$k_z = k_0 \cos \theta.$$

At $z = 0$, the following relation from the boundary condition on the x component of the electric field results:

$$E_0 \cos \theta e^{-jk_0 x \sin \theta} = \frac{H'_0 k'_z}{\omega\epsilon_p} [1 - \Gamma] e^{-jk'_x x}.$$

Since the relation must hold for any x , then

$$k_0 \sin \theta = k'_x = k_p \sin \theta'$$

and

$$E_0 \cos \theta = \frac{H'_0 k'_z}{\omega\epsilon_p} [1 - \Gamma]. \quad (2.28)$$

From the boundary conditions at $z = 1$, the following relations are obtained:

$$H_0 e^{-jk_z l} = H'_0 \left[e^{-jk'_z l} + \Gamma e^{jk'_z l} \right] \quad (2.29)$$

and

$$H_0 \frac{k_z}{\omega \epsilon_0} e^{-jk_z l} = \frac{H'_0 k'_z}{\omega \epsilon_p} \left[e^{-jk'_z l} - \Gamma e^{jk'_z l} \right] \quad (2.30)$$

There are three equations (2.28), (2.29), and (2.30), and three unknowns H'_0 , H_0 and Γ . Solving for H_0 :

$$H_0 = E_0 \sqrt{\frac{\epsilon_0}{\mu_0}} e^{jk_z l} \left[\frac{1}{\cos k'_z l + j \frac{k'_z \epsilon_0}{k_z \epsilon_p} \sin k'_z l} \right] \quad (2.31a)$$

Thus the amplitude of the magnetic field in the free space region is given by:

$$|h_y| = \frac{\sqrt{\frac{\epsilon_0}{\mu_0}} E_0}{\left[\cos^2 k'_z l + \frac{k'^2_z \epsilon_0^2}{k_z^2 \epsilon_p^2} \sin^2 k'_z l \right]^{\frac{1}{2}}} \quad (2.31b)$$

The interesting part of this result is that as far as the θ dependence is concerned, the expression for H_0 is exactly the same as the far-field pattern obtained for the narrow slit case [see Eq. (2.22)]. The similarity of the results suggests interpretations for some features of the power patterns in terms of the plane wave model. However, in order to make the interpretations easier, analogies can be drawn with the transmission line.

The transmission line analogue of the plane wave model is found to be as shown in Figure 10. (See Reference 4 for transmission line analogues of plane waves.)

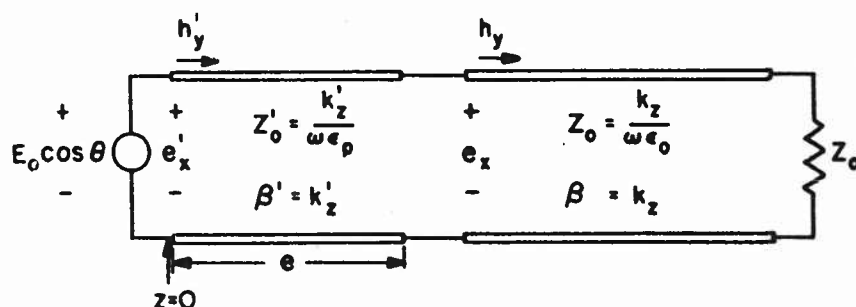


Figure 10. Transmission Line Analogue

The analogue gives the z variation of the field components e'_x, h'_y, e_x and h_y . If the system is solved for h_y , then

$$h_y = E_0 \sqrt{\frac{\epsilon_0}{\mu_0}} \frac{e^{-jk_z(z-1)}}{\left[\cos k'_z l + j \frac{k'_z \epsilon_0}{k_z \epsilon_p} \sin k'_z l \right]} .$$

The power propagated per unit area can be computed from

$$p = \frac{1}{2} \sqrt{\frac{\mu_0}{\epsilon_0}} |h_y|^2 .$$

When $e = 0$, then

$$|h_y| = E_0 \sqrt{\frac{\epsilon_0}{\mu_0}} .$$

Let us investigate the peaking effect observed in Figures 6 and 7. It should be noted that these peaks are greater in amplitude than the case without the plasma slab.

From Eq. (2.31),

$$|h_y| = E_0 \sqrt{\frac{\epsilon_0}{\mu_0}} \left[\frac{1}{1 - \left(1 - \frac{k'^2_z \epsilon_0}{k_z^2 \epsilon_p} \right) \sin^2 k'_z l} \right]^{\frac{1}{2}} .$$

Thus $|h_y|$ can become greater than $E_0 \sqrt{\frac{\epsilon_0}{\mu_0}}$ when

$$0 < \frac{k'_z \epsilon_0}{k_z \epsilon_p} < 1 .$$

This condition is indeed satisfied in the range

$$\sin^{-1} \left(\frac{\epsilon_p}{\epsilon_p + \epsilon_0} \right) < \theta < \theta_c$$

and within this range of angles, the power radiated is greater than the "no plasma" case.

Similar relations are obtained for H_y in the narrow slit problem [see Eq. (2.22)] .

In terms of the transmission line analogue, the condition

$$\frac{k'_z \epsilon_0}{k_z \epsilon_p} < 1$$

is analogous to

$$\frac{Z'_0}{Z_0} < 1$$

or

$$Z'_0 < Z_0 .$$

By adding a transmission line of lower characteristic impedance to a matched line, the impedance seen from the source is always reduced. Hence, more power is delivered to the load.

The transmission line analogy also shows why fluctuations in the power pattern for thick plasma layers are observed. As θ changes from 0 to θ_c , the propagation constant k'_z in the transmission line analogue changes from k_p to 0. Thus when $k_p l \gg 1$, the length l changes from many wavelengths to zero wavelength as θ is changed from 0 to θ_c . In other words, the impedance seen from the source fluctuates as θ is varied and fluctuations in the power pattern result.

When the angle θ is greater than θ_c or when $\frac{\omega_p}{\omega} > 1$, the transmission line analogy no longer holds. In such a case, the plane waves within the plasma layer are non-uniform and are attenuated in the z direction.

3. TRANSVERSE ELECTRIC WAVE

3.1 Solution

Now consider the case of the electric field polarized along the gap in y direction. The geometry for this problem is shown in Figure 11. The field-strength distribution across the gap is assumed to be co-sinusoidal as shown in Figure 12. This particular configuration corresponds to a waveguide opening into half space with the waveguide excited by TE_{10} mode.

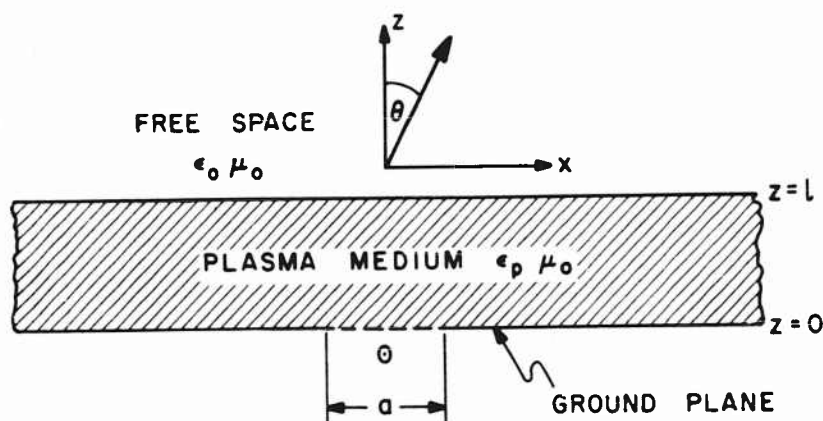


Figure 11. Radiative Geometry for the TE Wave Case

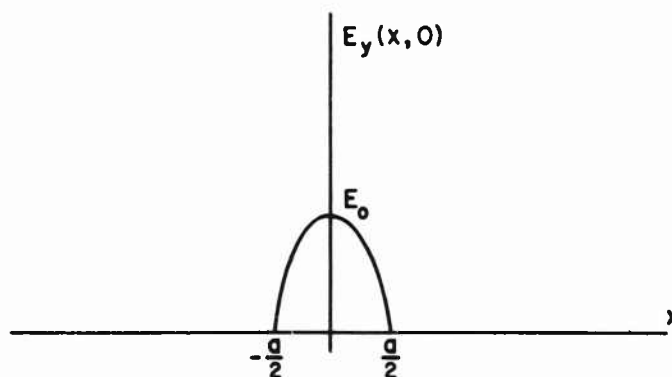


Figure 12. Electric Field Amplitude Distribution at $z = 0$ for the TE Wave Case

The method used to solve this problem is very similar to the one used in the previous problem. In this particular polarization and geometry, it can be seen that

$$\begin{aligned} E_x &= E_z = H_y = 0 \\ E'_x &= E'_z = H'_y = 0 \end{aligned}$$

There is only one component of electric field and in the free space it is represented by the following integral:

$$E_y(x, z) = \int_{-\infty}^{\infty} a(k_x) e^{-j(k_x x + k_z z)} dk_x \quad (3.1)$$

The solution above is identical to the one assumed in the previous problem except this time the solution is assumed for the electric instead of magnetic field. The corresponding magnetic field components in free space region are given by the following relations:

$$H_x(x, z) = \frac{1}{j\omega\mu_0} \frac{\partial E_y}{\partial z} = - \int_{-\infty}^{\infty} \frac{k_z}{\omega\mu_0} a(k_x) e^{-j(k_x x + k_z z)} dk_x \quad (3.2)$$

and

$$H_z(x, z) = \frac{1}{j\omega\mu_0} \frac{\partial E_y}{\partial x} = \int_{-\infty}^{\infty} \frac{k_x}{\omega\mu_0} a(k_x) e^{-j(k_x x + k_z z)} dk_x \quad (3.3)$$

Inside the plasma medium, the solution is represented in terms of outgoing waves and reflected waves:

$$E'_y(x, z) = \int_{-\infty}^{\infty} \left[b(k'_x) e^{-jk'_z z} + c(k'_x) e^{jk'_z z} \right] e^{-jk'_x x} dk'_x \quad (3.4)$$

and the corresponding magnetic field is given by:

$$\begin{aligned} H'_x(x, z) &= \frac{1}{j\omega\mu_0} \frac{\partial E'_y}{\partial z} \\ &= - \int_{-\infty}^{\infty} \frac{k'_z}{\omega\mu_0} \left[b(k'_x) e^{-jk'_z z} - c(k'_x) e^{jk'_z z} \right] e^{-jk'_x x} dk'_x \end{aligned} \quad (3.5)$$

$$\begin{aligned}
H'_z(x, z) &= \frac{-1}{j\omega\mu_0} \frac{\partial E_y}{\partial x} \\
&= \int_{-\infty}^{\infty} \frac{k'_x}{\omega\mu_0} \left[b(k'_x) e^{-jk'_z z} + c(k'_x) e^{jk'_z z} \right] e^{-jk'_x x} dk'_x.
\end{aligned} \tag{3.6}$$

At the ground plane the tangential component of electric field, $E'_y(x, 0)$, must be 0 everywhere except at the gap where the amplitude distribution becomes co-sinusoidal as discussed earlier. Equation (3.4) for the electric field becomes at the ground plane:

$$E'_y(x, 0) = \int_{-\infty}^{\infty} \left[b(k'_x) + c(k'_x) \right] e^{-jk'_x x} dk'_x \tag{3.7}$$

which indicates that the quantity

$$b(k'_x) + c(k'_x)$$

is the Fourier transform of the co-sinusoidal electric field amplitude distribution. By equating the Fourier transform to the expression above, then

$$\left[b(k'_x) + c(k'_x) \right] = \frac{2\pi E_0 \cos k'_x \frac{a}{2}}{\left(\frac{\pi}{a} \right)^2 - k'^2_x} \tag{3.8}$$

Equation (3.8) gives one of the three required relations to solve for $a(k'_x)$.

At the interface between the plasma and the free space continuity, conditions on the tangential components of electric and magnetic fields result. Thus, the two electric fields $E'_y(x, 1)$ and $E_y(x, 1)$ are equated and also the two magnetic fields $H'_x(x, 1)$ and $H_x(x, 1)$. In equating them, it can be seen again that k'_x must be equal to k_x . The equality provides the equation of the quantities inside the integral as in the previous problem.

By equating Eqs. (3.1) and (3.4) at $z = 1$, then

$$a(k_x) e^{-jk_z 1} = b(k'_x) e^{-jk'_z 1} + c(k'_x) e^{jk'_z 1} \tag{3.9}$$

for the electric field continuity. For the magnetic field continuity relation, from Eqs. (3.2) and (3.5) results

$$k_z a(k_x) e^{-jk_z 1} = k'_z \left[b(k'_x) e^{-jk'_z 1} - c(k'_x) e^{jk'_z 1} \right] \tag{3.10}$$

Equations (3.8), (3.9) and (3.10) give three equations and three unknowns

enabling us to solve for $a(k_x)$. By solving the equations for $a(k_x)$, there results

$$a(k_x) = \frac{2\pi E_0 \cos k'_x \frac{a}{2}}{\left(\frac{\pi}{a}\right)^2 - k_x'^2} \left[\frac{e^{jk_z' l}}{\cos k_z' l + j \frac{k_z}{k_z'} \sin k_z' l} \right] \quad (3.11)$$

As before, Snell's law allows the quantities k'_x , k'_z and k_z' to be expressed in terms of k_x .

The far-field approximate expression for the electric field can be obtained by the saddle-point method, and the result is as follows:

$$E_y \approx \sqrt{\frac{2\pi}{k_0 r}} e^{j\pi/4} k_0 \cos \theta a(k_0 \sin \theta) e^{-jk_0 r} \quad (3.12)$$

where

$$k_0 r \gg 1.$$

If Eq. (3.11) is used to evaluate $a(k_0 \sin \theta)$, the following substitutions can be used:

$$k_x = k'_x = k_0 \sin \theta$$

$$k_z = k_0 \cos \theta$$

$$k'_z = \left[k_p^2 - k_0^2 \sin^2 \theta \right]^{\frac{1}{2}}$$

3.2 Results

The normalized power pattern can be obtained from the relation

$$p = \frac{1}{2} \sqrt{\frac{\epsilon_0}{\mu_0}} |E_y|^2$$

Again, only the lossless case is considered. In the lossless case, the quantity k'_z takes on either real or imaginary values as in the case of the transverse magnetic wave studied in the previous section. Thus two expressions are given for the power pattern.

Let

$$k'_{zr} = \left[k_p^2 - k_0^2 \sin^2 \theta \right]^{\frac{1}{2}} \quad \text{for } k_p > k_0 \sin \theta$$

and

$$k'_{zi} = \left[k_0^2 \sin^2 \theta - k_p^2 \right]^{\frac{1}{2}} \quad \text{for } k_p < k_0 \sin \theta ,$$

where

$$k_p = k_0 \left[1 - \frac{\omega_p^2}{\omega^2} \right]^{\frac{1}{2}}$$

Then the following expressions for the power pattern can be obtained from Eqs. (3.11) and (3.12). The power is normalized so that the electric field amplitude between the slit is kept constant for all cases. Furthermore, the value of $\frac{1}{r}$ is given to the power radiated in $\theta = 0$ direction for the "no plasma" case.

$$P_n = \frac{1}{r} \left(\frac{\pi}{a} \right)^4 \left[\frac{\cos \left(\frac{k_0 a}{2} \sin \theta \right)}{\left(\frac{\pi}{a} \right)^2 - k_0^2 \sin^2 \theta} \right]^2 \left[\frac{\cos^2 \theta}{\cos^2 k'_{zr} l + \frac{k_0^2 \cos^2 \theta}{k'^2_{zr}} \sin^2 k'_{zr} l} \right] \quad (3.13a)$$

for

$$k_p > k_0 \sin \theta ,$$

and

$$P_n = \frac{1}{r} \left(\frac{\pi}{a} \right)^4 \left[\frac{\cos \left(\frac{k_0 a}{2} \sin \theta \right)}{\left(\frac{\pi}{a} \right)^2 - k_0^2 \sin^2 \theta} \right]^2 \left[\frac{\cos^2 \theta}{\cosh^2 k'_{zi} l + \left(\frac{k_0 \cos \theta}{k'_{zi}} \right)^2 \sinh^2 k'_{zi} l} \right] \quad (3.13b)$$

for

$$k_p < k_0 \sin \theta .$$

If the plasma layer is lossy, it is necessary to use

$$k_p = k_0 \left[1 + \frac{\omega_p^2}{(\nu + j\omega)j\omega} \right]^{\frac{1}{2}}$$

to obtain k'_{z} . In such a case, k'_{z} is complex and a simple expression for power cannot be obtained. However, the exact expressions for the lossy plasma case are given in the Appendix.

For the particular electric field polarization considered in this section, radiation from an infinitesimally narrow slot is not possible. Thus, for the calculation of the radiation pattern, a value of .8 was assigned to $\frac{a}{\lambda}$, the ratio of slot width to free space wavelength. The value assigned is a typical value for the ratio of waveguide width to free space wavelength for a TE_{10} waveguide mode.

The radiation patterns are shown in Figures 13 and 14. Unlike the transverse magnetic case treated in the previous section, the power pattern without the plasma layer is not omni-directional.

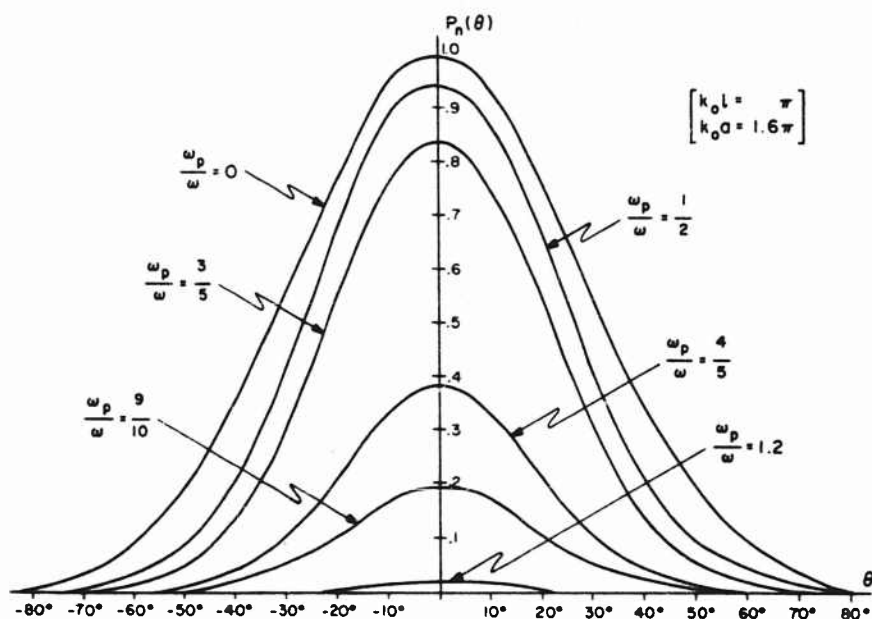


Figure 13. Power Patterns for Various Values of $\frac{\omega_p}{\omega}$ (TE Wave Case)

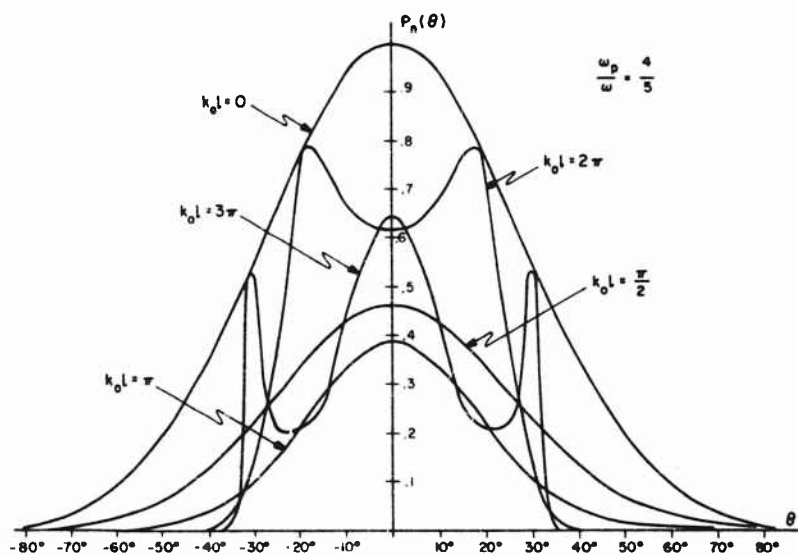


Figure 14. Power Patterns for Various Values of $k_0 l$ (TE Wave Case)

Again, analogies with the transmission line can be drawn as was done in Section 2. However, the characteristic impedances of the equivalent transmission lines must be re-defined. For instance, it is necessary to identify Z_0 with $\frac{\omega\mu_0}{k_z}$ instead of $\frac{k_z}{\omega\epsilon_0}$. (See Figure 10 and the subsequent analysis.)

Since the quantity k_z/k'_z in the denominator of Eq. (3.13a) is always greater than unity for real values of k'_z , the radiated power never exceeds that of the "no plasma" case. As a result, peaks are observed whenever $k'_z l = n\pi$ where n is a non-zero integer. Whenever $k_p l < \pi$, the only peak is the one at $\theta = 0$ and the power pattern decreases monotonically with θ .

4. ANISOTROPIC PLASMA

4.1 Introduction

In the presence of a magnetostatic field, the plasma medium becomes anisotropic.^{8,9} In general, with the magnetostatic field in the z direction in a right-hand rectangular coordinate system, the relative dielectric permittivity can be described by the following tensor (see Section 1.2).

$$\begin{bmatrix} 1 + \frac{\nu + j\omega}{(\nu + j\omega)^2 + \omega_b^2} \left(\frac{\omega_p^2}{j\omega} \right) & \frac{\omega_b}{(\nu + j\omega)^2 + \omega_b^2} \left(\frac{\omega_p^2}{j\omega} \right) & 0 \\ \frac{-\omega_b}{(\nu + j\omega)^2 + \omega_b^2} \left(\frac{\omega_p^2}{j\omega} \right) & 1 + \frac{(\nu + j\omega)}{(\nu + j\omega)^2 + \omega_b^2} \left(\frac{\omega_p^2}{j\omega} \right) & 0 \\ 0 & 0 & 1 + \frac{\omega_p^2}{(\nu + j\omega)(j\omega)} \end{bmatrix}.$$

Because the off diagonal elements of the tensor are complex quantities, the electromagnetic waves in such a medium propagate in a very complex manner. Thus only the special case of a very high magnetostatic field is studied.

When the magnetostatic field becomes very high, the dielectric tensor approaches the following expression:

$$\begin{bmatrix} \epsilon_0 & 0 & 0 \\ 0 & \epsilon_0 & 0 \\ 0 & 0 & \epsilon_0 \left[1 + \frac{\omega_p^2}{(\nu + j\omega)(j\omega)} \right] \end{bmatrix}.$$

The off diagonal elements go to 0 and the only remaining element different from the free space permittivity is the one associated with the direction of the magnetostatic field vector.

In the analysis to follow, it is assumed that the magnetostatic field is strong enough so that the above tensor is a valid representation.

4.2 Propagation in Anisotropic Medium

At this point, an investigation of electromagnetic wave propagation in an anisotropic medium is appropriate.

Consider the geometry shown in Figure 15. The space is filled with

an anisotropic dielectric which can be described by a dielectric tensor of the following form:

$$\begin{bmatrix} \epsilon_x & 0 & 0 \\ 0 & \epsilon_y & 0 \\ 0 & 0 & \epsilon_z \end{bmatrix}$$

Assume that a uniform plane wave travels in the θ direction and perpendicular to the y axis, and that the magnetic field is polarized in the y direction.

Since the medium is non-gyrotropic, this configuration is as follows:

$$H_x = H_z = E_y = 0.$$

From the equation

$$\nabla \times \vec{H} = j\omega \underline{\underline{\epsilon}} \vec{E},$$

we obtain the relations

$$E_x = \frac{-1}{j\omega \epsilon_x} \frac{\partial H_y}{\partial z} \quad (4.1)$$

and

$$E_z = \frac{1}{j\omega \epsilon_z} \frac{\partial H_y}{\partial x}. \quad (4.2)$$

The other curl equation

$$\nabla \times \vec{E} = -j\omega \mu_0 \vec{H}$$

yields the following relation:

$$H_y = \frac{-1}{j\omega \mu_0} \left[\frac{\partial E_x}{\partial z} + \frac{\partial E_z}{\partial x} \right]. \quad (4.3)$$

By substituting Eqs. (4.1) and (4.2) into (4.3), the following partial differential equation for H_y is derived:

$$H_y = \frac{-1}{\omega^2 \mu_0} \left[\frac{1}{\epsilon_x} \frac{\partial^2 H_y}{\partial z^2} + \frac{1}{\epsilon_z} \frac{\partial^2 H_y}{\partial x^2} \right]. \quad (4.4)$$

The general solution to such an equation is given by:

$$H_y = A \left(e^{-jk_x x} + R_1 e^{jk_x x} \right) \left(e^{-jk_z z} + R_2 e^{jk_z z} \right)$$

which, when substituted back into the equation, gives:

$$\frac{k_z^2}{\omega^2 \mu_0 \epsilon_x} + \frac{k_x^2}{\omega^2 \mu_0 \epsilon_z} = 1 \quad (4.5)$$

Equation (4.5) is the relation that must hold between k_x and k_z in the mode of propagation considered.

The propagation constant k , as a function of θ , can be obtained by substituting $k_x = k \sin \theta$ and $k_z = k \cos \theta$ into Eq. (4.5). It is found that

$$k = \left[\frac{\epsilon_x \epsilon_z \omega^2 \mu_0}{\epsilon_x \cos^2 \theta + \epsilon_z \sin^2 \theta} \right]$$

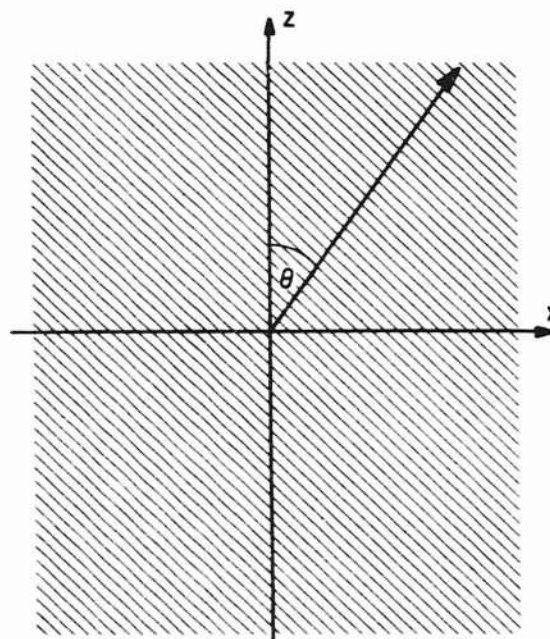


Figure 15. Plane Wave in Anisotropic Medium

4.3 Solution

The problem of finding the radiation pattern with the anisotropic plasma is approached in much the same way as in the previous cases. It is seen that there are only two interesting configurations. In both cases, the polarization of the electric field at the gap is in the x direction as in the problem of Section 2. In one case, the magnetostatic field vector is in the z direction, and in the other, it is in the x direction. Any other combination of magnetostatic field direction and electric field polarization reduces either to the case with no plasma or to the case already studied due to the fact that two of the diagonal elements of the tensor have the value of ϵ_0 . Thus, only the two cases mentioned are considered.

The geometry and the excitation of this problem are the same as described in Figures 2 and 3. Since the plasma medium is non-gyrotropic, it is expected that

$$H_x = H_z = E_y = 0$$

$$H'_x = H'_z = E'_y = 0$$

assuming of course that the magnetostatic field points either in x or z direction. As before, the solution for magnetic field in free space is assumed to be of the following form:

$$H_y = \int_{-\infty}^{\infty} a(k_x) e^{-j(k_x x + k_z z)} dk_x \quad (4.6)$$

with the corresponding electric field components

$$E_z = - \int_{-\infty}^{\infty} \frac{k_x}{\omega \epsilon_0} a(k_x) e^{-j(k_x x + k_z z)} dk_x, \quad (4.7)$$

and

$$E_x = \int_{-\infty}^{\infty} \frac{k_z}{\omega \epsilon_0} a(k_x) e^{-j(k_x x + k_z z)} dk_x. \quad (4.8)$$

Inside the plasma medium, a solution identical to the one assumed in Eq. (2.4) of Section 2 is assumed for the magnetic field as shown:

$$H'_y = \int_{-\infty}^{\infty} \left[b(k'_x) e^{-jk'_z z} + c(k'_x) e^{jk'_z z} \right] e^{-jk'_x x} dk'_x. \quad (4.9)$$

However, this time it must be noted that there is a different relation between k'_x and k'_z , namely;

$$\frac{k'^2_x}{\omega^2 \mu_0 \epsilon_z} + \frac{k'^2_z}{\omega^2 \mu_0 \epsilon_x} = 1 \quad (4.10)$$

The electric field in the plasma medium is given by:

$$E'_x = \int_{-\infty}^{\infty} \frac{k'_z}{\omega \epsilon_x} \left[b(k'_x) e^{-jk'_z z} - c(k'_x) e^{jk'_z z} \right] e^{-jk'_x x} dk'_x \quad (4.11)$$

and

$$E'_z = \int_{-\infty}^{\infty} \frac{k'_x}{\omega \epsilon_z} \left[b(k'_x) e^{-jk'_z z} + c(k'_x) e^{jk'_z z} \right] e^{-jk'_x x} dk'_x \quad (4.12)$$

The procedure henceforth for finding $a(k'_x)$ is exactly as that in Section 2, and thus a detailed analysis is omitted. The Fourier transform technique is used to match the boundary conditions. As before, the continuity conditions on the electric and the magnetic fields yield Snell's law giving the relation, $k_x = k'_x$.

The resulting function, $a(k'_x)$, is identical to Eq. (2.13) except that ϵ_p is replaced by ϵ_x .

$$a(k'_x) = \frac{2\pi E_0 a \sin(k'_x \frac{a}{2})}{k_z (k'_x \frac{a}{2})} \left[\frac{c k'_z}{\cos k'_z l + j \frac{k'_z \epsilon_0}{k'_z \epsilon_x} \sin k'_z l} \right] \quad (4.13)$$

From the relation $k_x = k'_x$, k'_z can be evaluated in terms of k_x using Eq. (4.9) to get

$$k'_z = \left(\omega^2 \mu_0 \epsilon_x \left[1 - \frac{k_x^2}{\omega^2 \mu_0 \epsilon_z} \right] \right)^{\frac{1}{2}} \quad (4.14)$$

The values of ϵ_x and ϵ_z depend on the direction of the magnetostatic field vector. The relation between k_x and k_z is given by:

$$k_z = (\omega^2 \mu_0 \epsilon_0 - k_x^2)^{\frac{1}{2}} \quad (4.15)$$

Thus, $a(k'_x)$ can be expressed entirely in terms of k_x .

By applying the saddle-point method, the far-field pattern is obtained and is as shown below:

$$H_y \approx \sqrt{\frac{2\pi}{k_0 r}} k_0 \cos \theta a(k_0 \sin \theta) e^{-j(k_0 r - \frac{\pi}{4})} \quad (4.16)$$

The quantity $a(k_0 \sin \theta)$ can be evaluated using Eq. (4.13) and the auxiliary relations in Eqs. (4.14) and (4.15).

4.4 Results

In the following analysis, it is assumed that the plasma layer is lossless. The power pattern for the lossy case can be obtained by substituting the proper values of ϵ_x and ϵ_z into Eqs. (4.13), (4.14), (4.15), and (4.16).

(a) Magnetostatic field vector in the z direction

When the magnetostatic field is z directed, then

$$\begin{aligned} \epsilon_x &= \epsilon_0 \\ \epsilon_z &= \epsilon_0 \left[1 - \frac{\omega_p^2}{\omega^2} \right] \end{aligned}$$

By substituting these quantities into Eq. (4.14) and setting $k_x = k_0 \sin \theta$, there results

$$k'_z = k_0 \left[\frac{\cos^2 \theta - \frac{\omega_p^2}{\omega^2}}{1 - \frac{\omega_p^2}{\omega^2}} \right]^{\frac{1}{2}} \quad (4.17)$$

The expression above shows that when $\frac{\omega_p}{\omega}$ is greater than unity, k'_z is always real. However, when $\frac{\omega_p}{\omega} < 1$, k'_z takes on either real or imaginary values. Thus it is again convenient to obtain two expressions for the power pattern.

$$\text{Let } k'_{zr} = k_0 \left[\frac{\cos^2 \theta - \frac{\omega_p^2}{\omega^2}}{1 - \frac{\omega_p^2}{\omega^2}} \right]^{\frac{1}{2}} \quad \text{for } \cos \theta > \frac{\omega_p}{\omega}$$

and

$$k'_{zi} = k_0 \left[\frac{\frac{\omega_p^2}{\omega^2} - \cos^2 \theta}{1 - \frac{\omega_p^2}{\omega^2}} \right]^{\frac{1}{2}} \quad \text{for } \cos \theta < \frac{\omega_p}{\omega} < 1$$

By using these relations with Eqs. (4.13) to (4.16), the following expressions

for the normalized power pattern are obtained:

$$P_n = \frac{1}{r} \left[\frac{\sin(\frac{k_0 a}{2} \sin \theta)}{\frac{k_0 a}{2} \sin \theta} \right]^2 \left[\frac{1}{\cosh^2 k'_{zi} + \left(\frac{k'_{zi}}{k_0 \cos \theta} \right)^2 \sinh^2 k'_{zi}} \right] \quad (4.18)$$

for

$$\cos \theta < \frac{\omega_p}{\omega} < 1$$

and

$$P_n = \frac{1}{r} \left[\frac{\sin(\frac{k_0 a}{2} \sin \theta)}{\frac{k_0 a}{2} \sin \theta} \right]^2 \left[\frac{1}{\cos^2 k'_{zr} + \left(\frac{k'_{zr}}{k_0 \cos \theta} \right)^2 \sin^2 k'_{zr}} \right] \quad (4.19)$$

for

$$k'_z = \text{real number.}$$

Equations (4.13) and (4.19) give the power pattern for the case of infinite magnetostatic field directed parallel to the z axis.

The radiation patterns as function of $\frac{\omega_p}{\omega}$ are shown in Figure 5. It is assumed that the slot is infinitesimally narrow. Qualitatively the patterns are quite similar to those in Figure 5, the case of no magnetic field. However, unlike the patterns of Figure 5, the peaks are higher for larger values of $\frac{\omega_p}{\omega}$ and the normalized power is unity in the direction of the magnetostatic field even when $\frac{\omega_p}{\omega}$ is greater than unity. This latter effect is expected because the propagation constant in the direction of magnetostatic field reduces to that of the free space. The wave traveling in this direction has its electric field polarized perpendicular to the direction of the magnetostatic field. Since the dielectric permittivity associated with the direction perpendicular to the magnetostatic field is ϵ_0 , the wave propagates with the free space propagation constant.

(b) Magnetostatic field vector parallel to the x axis

Now consider the case of magnetostatic field parallel to the x axis. In this case,

$$\epsilon_x = \epsilon_0 \left(1 - \frac{\omega_p^2}{\omega^2} \right)$$

$$\epsilon_z = \epsilon_0$$

By substituting these relations into Eq. (4.14) and setting $k_x = k_0 \sin \theta$

$$k'_z = k_0 \cos \theta \left[1 - \frac{\omega_p^2}{\omega^2} \right]^{\frac{1}{2}}$$

Clearly, k'_z is real when $\frac{\omega_p}{\omega} < 1$ and is imaginary when $\frac{\omega_p}{\omega} > 1$.

Let

$$k'_{zr} = k_0 \cos \theta \left[1 - \frac{\omega_p^2}{\omega^2} \right]^{\frac{1}{2}} \quad \text{for } \frac{\omega_p}{\omega} < 1$$

and

$$k'_{zi} = k_0 \left[\frac{\omega_p^2}{\omega^2} - 1 \right] \cos \theta \quad \text{for } \frac{\omega_p}{\omega} > 1.$$

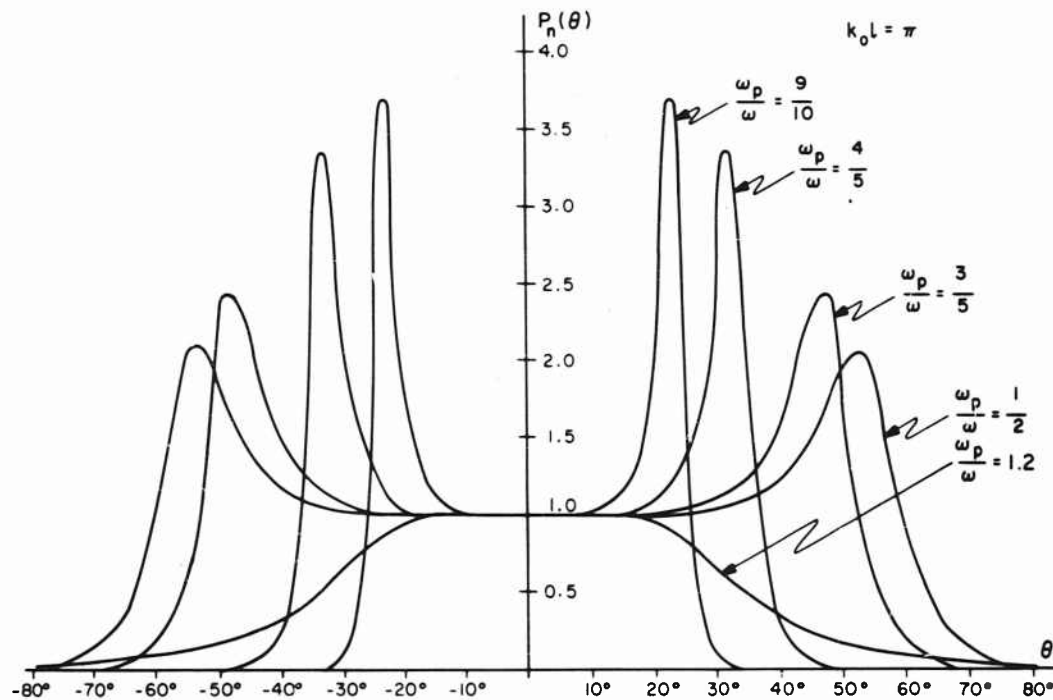


Figure 16. Power Patterns for Various Values of $\frac{\omega_p}{\omega}$ with the Magnetostatic Field in the z Direction

Then from Eqs. (4.13) to (4.16) the following expressions for the normalized power pattern are obtained:

$$P_n = \frac{1}{r} \left[\frac{\sin\left(\frac{k_0 a}{2} \sin \theta\right)}{\frac{k_0 a}{2} \sin \theta} \right]^2 \left[\frac{1}{\cos^2 k'_{zr} l + \left(\frac{1}{1 - \frac{\omega_p^2}{\omega^2}} \right) \sin^2 k'_{zr} l} \right] \quad (4.20a)$$

for $\frac{\omega_p}{\omega} < 1$

and

$$P_n = \frac{1}{r} \left[\frac{\sin\left(\frac{k_0 a}{2} \sin \theta\right)}{\frac{k_0 a}{2} \sin \theta} \right]^2 \left[\frac{1}{\cosh^2 k'_{zi} l + \left(\frac{1}{1 - \frac{\omega_p^2}{\omega^2}} \right) \sinh^2 k'_{zi} l} \right] \quad (4.20b)$$

for $\frac{\omega_p}{\omega} > 1$.

Shown in Figure 17 are the patterns with the magnetostatic field parallel to the x axis. Unlike the previous cases studied, power radiation is greatest along the ground plane. In addition, the amplitude never exceeds unity. As expected, the normalized power radiation is unity in the direction of the magnetostatic field.

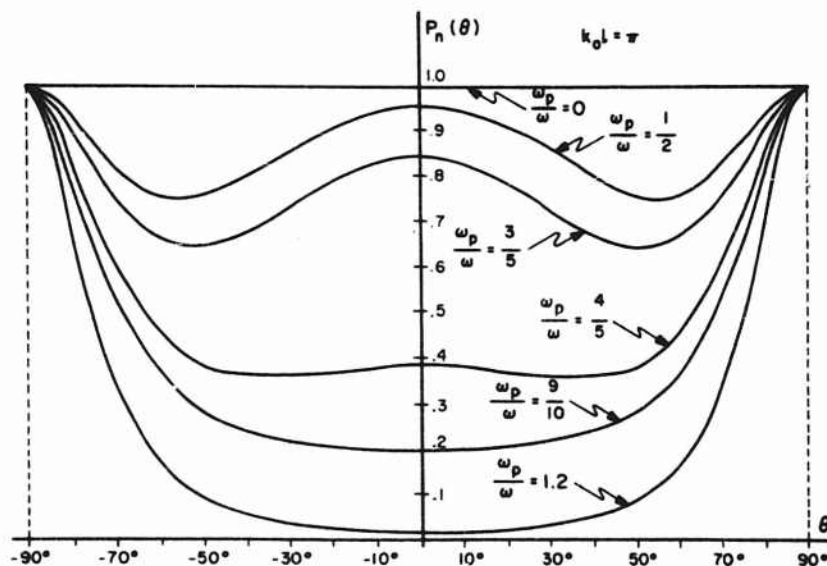


Figure 17. Power Patterns for Various Values of $\frac{\omega_p}{\omega}$ with the Magnetostatic Field in the x Direction

References

1. Walter Rotman, "Plasma Simulation by Artificial Dielectrics and Parallel Plate Media", IRE Trans. on Ants. and Prop., Vol. AP-10, No. 1, January 1962, pp. 82-95.
2. M. Newstein and J. Lurye, "The Field of a Magnetic Line-Source in the Presence of a Layer of Complex Refractive Index", Scientific Report No. 1 [Purchase Order SDP 40000 from G. E. Co. under Contract AFO4(645)-24], Technical Research Group, July 1956.
3. M. P. Bachynski, I. P. Shkarofsky, and T. W. Johnston, "Plasmas and the Electromagnetic Field", R. C. A. Victor Co., Ltd., Research Laboratories, Montreal, Canada.
4. R. B. Adler, L. J. Chu, and R. M. Fano, "Electromagnetic Energy Transmission and Radiation", (John Wiley and Sons, Inc., New York, 1960), Chap. 7.
5. G. N. Watson, "Theory of Bessel Functions", Cambridge University Press, 1944, pp. 235-240.
6. B. Noble, "Methods Based on the Wiener-Hopf Technique for the Solution of Partial Differential Equations", International Series of Monographs on Pure and Applied Mathematics, Vol. 7, (1958), pp. 27-37.
7. R. E. Collins, "Field Theory of Guided Waves", (McGraw-Hill Book Co., Inc., New York, 1960), pp. 495-506.
8. H. Hodara, H. R. Raemer, and G. I. Cohn, "Space Communication Problems During Re-entry", Paper Presented to the Chicago Chapter of the IRE, Professional Group on Space Electronics and Telemetry, February 12, 1960.
9. R. F. Whitmer, "Principles of Microwave Interactions with Ionized Media, Part II", Microwave Journal, March 1959, pp. 47-50.

Appendix

Radiation Patterns for Plasma Layers with Losses (No Static Magnetic Fields)

The power patterns for the lossy plasma layer can be derived from the general expressions for the transverse magnetic and electric wave cases [Eqs. (2.22) and (3.12) respectively] by allowing $\frac{\epsilon_p}{\epsilon_0}$ to become complex in accordance with Eq. (1.8). The following results are obtained after some algebraic manipulation:

(A) Transverse Magnetic Wave

(A1)

$$P_n = \frac{1}{r} \left[\frac{\sin(k_0 \frac{a}{2} \sin \theta)}{k_0 \frac{a}{2} \sin \theta} \right]^2 \cdot \frac{4(A^2 + B^2)}{C + D + E + F}$$

where $\frac{\epsilon_p}{\epsilon_0} = n^2 = A - jB$

$$C = e^{2\alpha l} \left[(Ak_0 \cos \theta + \beta)^2 + (Bk_0 \cos \theta + \alpha)^2 \right] \frac{1}{k_0^2}$$

$$D = e^{-2\alpha l} \left[(-Bk_0 \cos \theta + \alpha)^2 + (Ak_0 \cos \theta - \beta)^2 \right] \frac{1}{k_0^2}$$

$$E = 4 \sin 2\beta l \left[\alpha \beta - AB k_0^2 \cos^2 \theta \right] \frac{1}{k_0^2}$$

$$F = 2 \cos 2\beta l \left[A^2 k_0^2 \cos^2 \theta + B^2 k_0^2 \cos^2 \theta - \alpha^2 - \beta^2 \right] \frac{1}{k_0^2}$$

$$\alpha = k_0 \left[(A - \sin^2 \theta)^2 + B^2 \right]^{\frac{1}{4}} \sin \gamma$$

$$\beta = k_0 \left[(A - \sin^2 \theta)^2 + B^2 \right]^{\frac{1}{4}} \cos \gamma$$

$$\gamma = \frac{1}{2} \tan^{-1} \left(\frac{B}{A - \sin^2 \theta} \right)$$

(B) Transverse Electric Wave
(A2)

$$P_n = \left(\frac{\pi}{a} \right)^4 \left[\frac{\cos \left(k_0 \frac{a}{2} \sin \theta \right)}{\left(\frac{\pi}{a} \right)^2 - k_0^2 \sin^2 \theta} \right]^2 \frac{4 \cos^2 \theta [\alpha^2 + \beta^2]}{[C + D + E + F]}$$

where

$$\frac{\epsilon_p}{\epsilon_0} = n^2 = A - jB$$

$$C = e^{2\alpha l} \left[(\beta + k_0 \cos \theta)^2 + \alpha^2 \right]$$

$$D = e^{-2\alpha l} \left[(\beta - k_0 \cos \theta)^2 + \alpha^2 \right]$$

$$E = 2(\beta^2 + \alpha^2 - k_0^2 \cos^2 \theta) \cos 2\beta l$$

$$F = -4 \alpha k_0 \cos \theta \sin 2\beta l$$

$$\alpha = k_0 \left[(A - \sin^2 \theta)^2 + B^2 \right]^{\frac{1}{4}} \sin \gamma$$

$$\beta = k_0 \left[(A - \sin^2 \theta)^2 + B^2 \right]^{\frac{1}{4}} \cos \gamma$$

$$\gamma = \frac{1}{2} \tan^{-1} \left(\frac{B}{A - \sin^2 \theta} \right)$$

It should be noted that, since B is a positive number in the notations used, the following relation for γ holds:

$$0 \leq \gamma \leq \frac{\pi}{2}$$

<p>AF Cambridge Research Laboratories, Bedford, Mass. Electronic Research Directorate RADIATION PATTERN OF A SLIT IN A GROUND PLANE COVERED BY A PLASMA LAYER by M. Omura, December 1962. 48 pp. incl. tables, illus. AFCRL-62-958</p> <p>Expressions are obtained for radiation patterns of a slit in an infinite ground plane covered by a uniform layer of plasma. The slit is considered to be infinitely long. Two polarizations are considered: (1) the electric field is polarized across the gap and (2) along the slit. Effects of anisotropic plasmas on the radiation pattern are also studied; however only nongyrotropic plasmas are considered. Solutions to Maxwell's equations are expressed in terms of spectrum of plane waves in the rectangular coordinate system, and Fourier transform relations are used to match the boundary conditions. Solutions are in integral form, and the saddle-point integration method is used to obtain the far-field asymptotic expression of the solutions. Normalized power patterns are plotted for the various cases studied and the results discussed.</p>	<p>UNCLASSIFIED</p> <p>1. Plasma Physics 2. Electric Discharges 3. Radiation Pattern</p> <p>I. Omura, M.</p>	<p>AF Cambridge Research Laboratories, Bedford, Mass. Electronic Research Directorate RADIATION PATTERN OF A SLIT IN A GROUND PLANE COVERED BY A PLASMA LAYER by M. Omura, December 1962. 48 pp. incl. tables, illus. AFCRL-62-958</p> <p>Expressions are obtained for radiation patterns of a slit in an infinite ground plane covered by a uniform layer of plasma. The slit is considered to be infinitely long. Two polarizations are considered: (1) the electric field is polarized across the gap and (2) along the slit. Effects of anisotropic plasmas on the radiation pattern are also studied; however only nongyrotropic plasmas are considered. Solutions to Maxwell's equations are expressed in terms of spectrum of plane waves in the rectangular coordinate system, and Fourier transform relations are used to match the boundary conditions. Solutions are in integral form, and the saddle-point integration method is used to obtain the far-field asymptotic expression of the solutions. Normalized power patterns are plotted for the various cases studied and the results discussed.</p>	<p>UNCLASSIFIED</p> <p>1. Plasma Physics 2. Electric Discharges 3. Radiation Pattern</p> <p>I. Omura, M.</p>	<p>UNCLASSIFIED</p> <p>1. Plasma Physics 2. Electric Discharges 3. Radiation Pattern</p> <p>I. Omura, M.</p>	<p>UNCLASSIFIED</p> <p>1. Plasma Physics 2. Electric Discharges 3. Radiation Pattern</p> <p>I. Omura, M.</p>
<p>AF Cambridge Research Laboratories, Bedford, Mass. Electronic Research Directorate RADIATION PATTERN OF A SLIT IN A GROUND PLANE COVERED BY A PLASMA LAYER by M. Omura, December 1962. 48 pp. incl. tables, illus. AFCRL-62-958</p> <p>Expressions are obtained for radiation patterns of a slit in an infinite ground plane covered by a uniform layer of plasma. The slit is considered to be infinitely long. Two polarizations are considered: (1) the electric field is polarized across the gap and (2) along the slit. Effects of anisotropic plasmas on the radiation pattern are also studied; however only nongyrotropic plasmas are considered. Solutions to Maxwell's equations are expressed in terms of spectrum of plane waves in the rectangular coordinate system, and Fourier transform relations are used to match the boundary conditions. Solutions are in integral form, and the saddle-point integration method is used to obtain the far-field asymptotic expression of the solutions. Normalized power patterns are plotted for the various cases studied and the results discussed.</p>	<p>UNCLASSIFIED</p> <p>1. Plasma Physics 2. Electric Discharges 3. Radiation Pattern</p> <p>I. Omura, M.</p>	<p>AF Cambridge Research Laboratories, Bedford, Mass. Electronic Research Directorate RADIATION PATTERN OF A SLIT IN A GROUND PLANE COVERED BY A PLASMA LAYER by M. Omura, December 1962. 48 pp. incl. tables, illus. AFCRL-62-958</p> <p>Expressions are obtained for radiation patterns of a slit in an infinite ground plane covered by a uniform layer of plasma. The slit is considered to be infinitely long. Two polarizations are considered: (1) the electric field is polarized across the gap and (2) along the slit. Effects of anisotropic plasmas on the radiation pattern are also studied; however only nongyrotropic plasmas are considered. Solutions to Maxwell's equations are expressed in terms of spectrum of plane waves in the rectangular coordinate system, and Fourier transform relations are used to match the boundary conditions. Solutions are in integral form, and the saddle-point integration method is used to obtain the far-field asymptotic expression of the solutions. Normalized power patterns are plotted for the various cases studied and the results discussed.</p>	<p>UNCLASSIFIED</p> <p>1. Plasma Physics 2. Electric Discharges 3. Radiation Pattern</p> <p>I. Omura, M.</p>	<p>UNCLASSIFIED</p> <p>1. Plasma Physics 2. Electric Discharges 3. Radiation Pattern</p> <p>I. Omura, M.</p>	<p>UNCLASSIFIED</p> <p>1. Plasma Physics 2. Electric Discharges 3. Radiation Pattern</p> <p>I. Omura, M.</p>

AD	UNCLASSIFIED	AD	UNCLASSIFIED
AD	UNCLASSIFIED	AD	UNCLASSIFIED
AD	UNCLASSIFIED	AD	UNCLASSIFIED
AD	UNCLASSIFIED	AD	UNCLASSIFIED